ELECTRICAL MUSCLE STIMULATION PROTOCOLS: EFFECTS ON FORCE PRODUCTION AND ENERGY METABOLISM OF THE GASTROCNEMIUS MUSCLE IN HUMANS

By

ROBERT JAMES DUNLOP

B.P.E., The University of Alberta, 1986
B.Sc. P.T., The University of Alberta, 1987

A THESIS SUBMITTED IN PARTIAL FULFILLMENT OF

THE REQUIREMENTS FOR THE DEGREE OF

MASTER OF PHYSICAL EDUCATION

in

THE FACULTY OF GRADUATE STUDIES

Department of Sports Science
School of Physical Education

We accept this thesis as conforming

to the required standard

THE UNIVERSITY OF BRITISH COLUMBIA

May 1991

In presenting this thesis in partial fulfilment of the requirements for an advanced degree at the University of British Columbia, I agree that the Library shall make it freely available for reference and study. I further agree that permission for extensive copying of this thesis for scholarly purposes may be granted by the head of my department or by his or her representatives. It is understood that copying or publication of this thesis for financial gain shall not be allowed without my written permission.

Department of Sport Science

The University of British Columbia
Vancouver, Canada

Date May 27/91

DE-6 (2/88)

ABSTRACT

Electrical Muscle Stimulation (EMS) is commonly used in rehabilitation medicine to promote strength gains in skeletal muscle. However, despite its widespread use, the physiological effects of alterations in many EMS application variables has yet to be investigated. The stimulation duty cycle (work:rest ratio) is commonly manipulated by clinicians, without any physiological rationale for the use of a particular protocol. Understanding the mechanical and metabolic response of stimulated muscle to manipulation of this application variable is necessary in order optimize the efficacy of EMS as a training stimulus.

To evaluate the metabolic and mechanical effects of two EMS protocols commonly utilized in rehabilitation, the gastrocnemius muscle of healthy male subjects (n=8) was stimulated via surface electrodes (Medtronic Respond II) using a 1:1 work/rest ratio (Protocol A-10 sec stim./10 sec off) or a 1:5 work/rest ratio (Protocol B-10 sec stim./50 sec off) for 12 repetitions.

Each subject was placed supine on a specially fabricated foot pedal ergometer situated in the bore of a Phillips 1.5 tesla NMR unit. Muscular force production was measured during stimulation at 0.5 second intervals via a load cell connected to the foot pedal by a glass fibre rod, and interfaced with a microcomputer for continuous data acquisition. Relative changes in [PCr], [Pi], [ATP] and intracellular pH (pH_i) were obtained during stimulation and recovery, by ^{31}P NMR spectroscopy using a 1.5 cm RF surface

antenna. The RF coil interrogated a 15cc hemispherical volume of tissue to a maximal depth of 1.5 cm.

Results showed that protocol A produced a 30.4±1.3% decline in muscular force production while protocol B yielded a significantly smaller (13±0.8% - P<.001) reduction in force following 12 stimulations. During protocol A [Pi]/[PCr] increased significantly from resting values (Protocol A=210%, P<0.05) during the first 6 stimulations however, this ratio actually decreased slightly in the last 6 stimulations of the protocol (189%). During protocol B only small changes in [Pi[/[PCr] (48%) occurred in the first 6 stimulations, with no changes occurring in the final 6 simulations. pH_i was significantly (P<.001) lower in protocol A following 12 stimulations (Protocol A=6.8±0.16, Protocol B=7.03±0.12). The decline in pH_i in protocol A was highly correlated with the decline in force production (R^2=0.95). In protocol B pH_i recovered slightly between stimulation 9 and 12. ATP concentrations dropped insignificantly during stimulation in both protocols (3±0.1%), with insignificant changes during rest and recovery.

These results show that the application of EMS in protocol A produces profound changes in the high energy phosphates and intracellular pH, accompanied by a 30% decline in force production. In contrast, protocol B produced a brief period of pH and force decline followed by a steady state period characterized by insignificant changes in Pi/PCr, pH, and force production. Both protocols exhibited an alteration in the pattern of Pi/PCr and force output changes between 2 and 3 minutes of stimulation, possibly induced by changes in peripheral blood flow.

Protocol A induced changes in force output, Pi/PCr and pH similar to those reported during heavy resisted voluntary exercise. For healthy muscle a 10 second stimulation/10 second rest protocol produces mechanical and metabolic changes that closely approximate maximal voluntary resisted exercise.

TABLE OF CONTENTS

	Page
Abstract	ii
List of Tables	vii
List of Figures	viii
Acknowledgements	x
Introduction	1
Methodology	5
Results	17
Discussion	38
Conclusion	50
References	51
Appendix	
1. Review of Literature	67
1.1 Electrical Muscle Stimulation	67
1.1.1 Current Parameters	71
1.1.2 Application Protocols	74
1.1.3 Efficacy of Electrical Muscle Stimulation	78
1.2 Energy Metabolism during EMS	79
1.2.1 Metabolic Response to EMS	84

1.2.2 Intermittent Contractions 86

1.2.3 Metabolism and Fatigue 87

1.2.4 Metaboliic Recovery 91

1.3 Nuclear Magnetic Resonance 93

1.3.1 Magnetic Nuclei 94

1.3.2 Magnetic Nuclei in a Magnetic Field 95

1.3.3 Relaxation 102

1.3.4 Chemical Shift 104

1.3.5 Localization 107

1.3.6 Limitations of NMR 107

2. Raw Data 109

LIST OF TABLES

Table		Page
1.	Numerical Data: Stimulation	18
2.	Numerical Data: 10 Second Rest Period	29
3.	Numerical Data: 10 & 50 Second Rest Protocol B	31
4.	Numerical Data: Recovery	36

LIST OF FIGURES

Figure		Page
1.	Kin Com Isokinetic Dynamometer	8
2.	Foot Pedal Ergometer	9
3.	Glass Fibre Rod Attachment	10
4.	Force Acquisition	14
5.	Force Changes During each Repetition	19
6.	Force Production per Stimulation	19
7.	Force Production /Relative Time	22
8.	Pi/PCr per Stimulation	23
9.	Pi/PCr / Relative Time	23
10.	pH per Stimulation	26
11.	pH Relative Time	26
12.	pH over Force Production: Protocol A	27
13.	pH over Force Production: Protocol B	27
14.	Pi/PCr Stimulation & Rest: Protocol A	32
15.	Pi/PCr Stimulation & Rest: Protocol B	32
16.	Pi/PCr 10 and 50 Second Rest: Protocol B	33

17. pH Stimulation & Rest: Protocol A 34

18. pH Stimulation & Rest: Protocol B 34

19. Pi/PCr Recovery 37

20. pH Recovery 37

21. Sum of Delta Values 39

22. Electrical Stimulation Waveform 74

23. Nuclear Alignment 95

24. Nuclear Energy Levels 97

25. Nuclear Precession 97

26. Net Magnetization Vector 98

27. H_1 Radiofrequency Pulse 99

28. Radiofrequency Induced Precession 100

29. 90 Degree Radiofrequency Pulse 101

30. Free Induced Decay 106

31. NMR Spectra 106

Acknowledgement

I view this thesis, and this degree, as the product of a unique opportunity. The academic and professional growth I experienced during my time at U.B.C. was due in large part to the teaching, support, and friendship provided by the staff of the Allan McGavin Sports Medicine Centre. I would like to thank Trish Hopkins, Ronald Mattison, and Clyde Smith for offering a fellowship in sports physical therapy, which provided a wealth of clinical knowledge, and a foundation for my academic pursuits. I would also like to thank Don McKenzie and Peter Allen for serving as patient and supportive committee members. I am indebted to Gord Matheson for his support, motivation, guidance and friendship.

Special thanks to the constants in my life, my Mother, Father, Grandfather, and Victoria, for skillfully combating a 'graduate student stress syndrome'.

INTRODUCTION

For thousands of years electrical currents have been applied to human tissues in an attempt to produce therapeutic effects [39]. Currently, physical therapists use electrical stimulation to relieve pain, increase blood flow, and induce contractions in both innervated and denervated skeletal muscle [6]. In addition, muscle physiologists make extensive use of electrical stimulation to activate muscle independent of central neural control [51].

Application of electrical currents to the body in an effort to induce contraction in muscle is termed electrical muscle stimulation (EMS). In rehabilitation EMS is frequently applied, via surface electrodes, to produce strong tetanic contractions in weak and atrophied muscle in an effort to increase the muscle's force producing capabilities [77].

For the purpose of this investigation, strength will be defined as the ability of a muscle to produce high contractile forces for brief time periods (less than 10 seconds). In the past decade, the use of EMS to promote strength gains in healthy athletes has been reported [58]. Current research indicates that EMS may be as effective as voluntary isometric exercise in developing strength in healthy and atrophied muscle [26, 61, 64, 71]. However, despite its widespread use, experimentally validated guidelines for optimal EMS treatment protocols is lacking [60]. If EMS is to be used and evaluated as a strengthening modality, the physiological effects of various application techniques must be systematically investigated.

The development of high muscle tension appears to be the critical stimulus for increasing muscular strength [5]. Therefore the majority of muscle training programs advocate short duration contractions above 50% of a maximal voluntary contraction (MVC) to promote an increase in the muscle's ability to produce high forces over short periods of time [30]. Fatigued or weakened muscle cannot generate sufficient tension to sustain repeated high intensity efforts. Thus, in principle, it appears that repeated high intensity contractions with interspersed rest periods provides the optimal stimulus for muscular strength development [5].

In a recent review of the mechanisms of muscle strength development, Enoka stated that the use of a duty (work/rest) cycle which minimized the effects of fatigue is important in the design of EMS strengthening programs [35]. This assertion is based in part on significant strength gains achieved during an EMS training study [92] which utilized a 1:12 work/rest ratio

Changes in both neural and metabolic mechanisms are thought to contribute to the decline in muscle force output observed during repeated electrically induced contractions. Repeated one second electrical stimulation of the adductor pollicus muscle with one half second rest periods for a total of 60 seconds produced a decline in force output identical to that observed during continuous stimulation for 60 seconds [31]. In contrast, rest periods of one and two seconds produces significantly less force decline over the same period [31]. Electromyographic (EMG) evaluation during these three stimulation protocols, with normal and occluded circulation, lead the authors to

hypothesize that local metabolic events were responsible for the changes in force decline associated with alterations in rest period [31].

Intracellular anaerobic energy sources are called upon to meet the high rate energy requirements of high intensity short term muscular contractions [99]. Activation of these metabolic pathways results in depletion of the muscle's phosphocreatine (PCr) stores, and a reduction in intracellular pH (pH_i) secondary to lactate accumulation. Both of these events have long been viewed as a major contributors to muscular fatigue [66]. Thus, understanding the relationship between changes in muscular force output, and intracellular metabolic events, induced by alterations in EMS application protocols is necessary when designing EMS strengthening programs.

To date, no systematic investigation of the metabolic and mechanical effects of changes in EMS application protocols commonly utilized in clinical rehabilitation has been conducted. Such information is obviously essential to provide the clinician with a scientific basis for the selection of EMS application protocols. The purpose of this study is to investigate the alterations in muscle force output and cellular metabolic response associated with manipulation of the work/rest ratio during electrical stimulation of healthy human muscle, using commonly employed rehabilitation protocols as a basis for comparison. The hypotheses are: i) in the skeletal muscle fibers of healthy humans the ratio of Pi/PCr will increase in a linear fashion during electrical stimulation, reflecting the steady state relationship between oxidative phosphorylation and exercise intensity, ii) as work/rest ratio increases, greater increases in Pi/PCr will be accompanied by non-linear decreases in intracellular pH, and iii) increases in Pi/PCr and decreases in pH associated with

increased work/rest ratio will be accompanied by a reduction in muscular force production during repeated contractions.

The delimitations of this investigation result from the selection of the sample population and electrical stimulation method. Due to the high costs associated with NMR spectroscopy the sample population was made up of six male subjects. In clinical practice EMS is commonly employed in the treatment of muscle atrophy secondary to musculoskeletal injury. However, variability of the atrophic response and dysfunction in the adjacent bony or tendinous structures may significantly effect the muscle response to high intensity EMS. Thus subjects without recent history of lower extremity pathology were selected.

The limitations of this investigation include; i) the use of an external apparatus measuring linear force, to represent muscle force and ii) the inability to ensure that no element of voluntary muscle contraction accompanied EMS induced contractions during data collection.

METHODOLOGY

2.1 Subjects

Six healthy untrained male volunteers (mean age 26.8 years) participated in this study. Volunteers were excluded from participation in the study if they: (i) possessed any systemic disorders contraindicating high intensity muscular contractions, or EMS, (ii) had sustained a musculoskeletal injury to their lower extremities in the past year, (iii) participated in high intensity anaerobic training on a regular basis, (iv) were claustrophobic (risk of anxiety when positioned in the narrow NMR body chamber) or, v) were unable to tolerate sufficient electrical current to produce a 40% MVC calf contraction. Subjects were required to sign an NMR screening form, and a consent form in accordance with procedures governing human experimentation at the Universities of Alberta and British Columbia.

2.2 Electrical Muscle Stimulation

The muscle stimulating current was supplied by a modified Respond II neuromuscular stimulator†. The manufacturer altered the frequency control, enabling the investigators to accurately select a range of specific frequencies from 3 to 40 hertz (Hz) The Respond II produces an asymmetrical balanced biphasic square wave with a 300 μsec. pulse width. Pulse frequency was set and maintained at 40 Hz throughout the investigation. All current parameters were validated using an

† Medtronic Inc, Missassauga Ont.

oscilloscope. Once activated the stimulator reached peak current output in 0.5 seconds.

The Respond II stimulator is purported to provide a constant current source, automatically adjusting voltage to provide a constant current flow at a given intensity setting, regardless of resistance. A pilot evaluation (utilizing an oscilloscope and a wide range of standard resistors) confirmed that the stimulator did indeed provide a constant current source over a range of physiological resistances (> 3000 ohms).

Three AA size alkaline batteries were used to power the stimulator, with new cells provided for stimulation of each subject. Pilot studies revealed that fresh cells provided constant current levels over the course of 25, 10 second EMS calf contractions within the magnetic field. Variability in the effect of the magnetic field on battery current output was minimized by placing the stimulator in a standard location, within the magnet, during the stimulation of all subjects.

Prior to electrode application the skin on the subjects medial calf was cleansed using alcohol prep swabs. Approximately 20 cc of electroconductive gel was then applied to two, seven by two centimeter carbon rubber electrodes[†]. The electrodes were then placed, approximately 10 centimetres apart, on the skin over the proximal and distal aspects of the medial head of the dominant gastrocnemius muscle. Following this procedure both electrodes were fixed in place by tape and kling bandage.

EMS pretests of each subject were conducted to determine optimal electrode placement, individual current tolerance, and their relationship

---

[†] Medtronic Inc, Missassauga Ont.

to force generated by a maximal voluntary contraction. Utilizing the procedure described above electrodes were applied to the calf and small adjustments in placement were made in an attempt to maximize subjective contraction intensity, while minimizing associated discomfort.

Following a twenty minute rest period each subject was positioned in sitting, with both knees fully extended, on a Kin-Com isokinetic dynamometer[¢]. The forefoot was placed on the resistance pad with the ankle stabilized in plantigrade.(figure 1) Each subject performed two, ten second maximal voluntary plantar flexor contractions followed by three maximal EMS induced contractions without a voluntary component. Subjects controlled current intensity with a rheostat type dial. During the EMS contractions subjects were encouraged to increase current intensity to produce the highest level of muscle contraction possible without any voluntary muscle activation. Peak and average isometric force output was recorded for each contraction. In each case 10 minutes of rest was provided between contractions. During data collection the intensity of the electrical current applied to each subject was determined by individual subject tolerance. Although each subject achieved an EMS contraction corresponding to greater that 40% of MVC, no external standard of current intensity was preset.

[¢] Chattex Corp., Chattanooga, TEN.

Figure 1
Kin-Com dynamometer

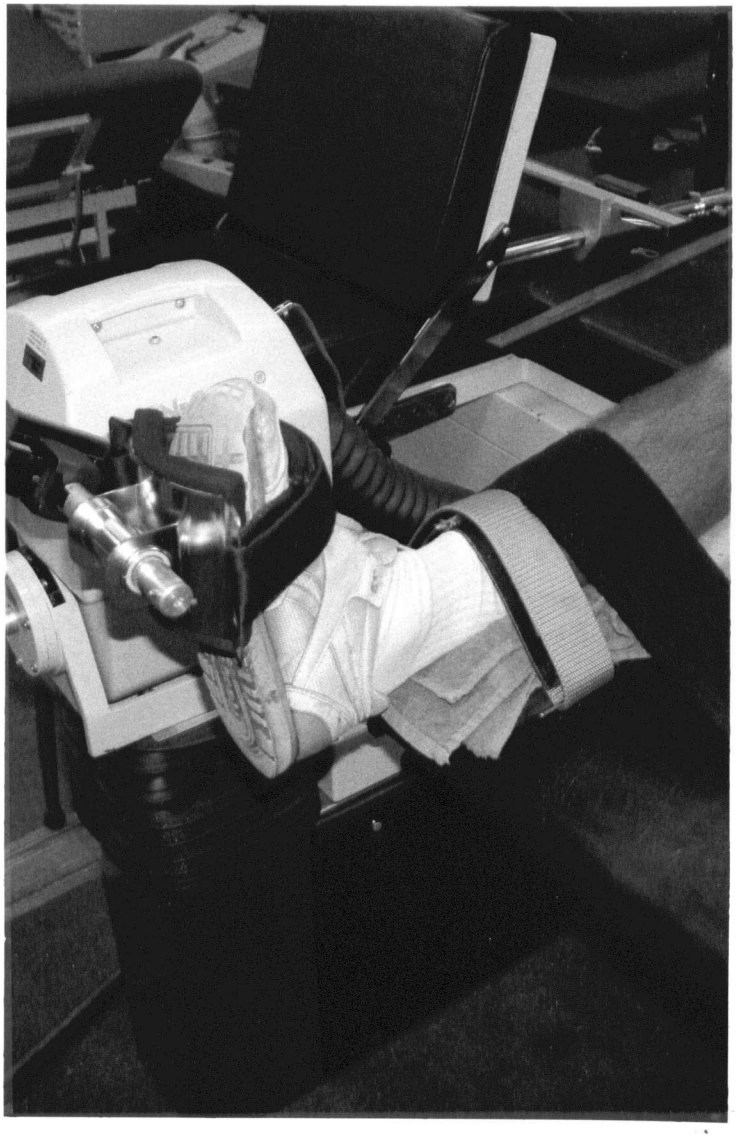

Isometric plantarflexion force (newtons) was recorded by a load cell mounted on the arm of the forefoot resistance pad

Figure 2
Foot Pedal Ergometer

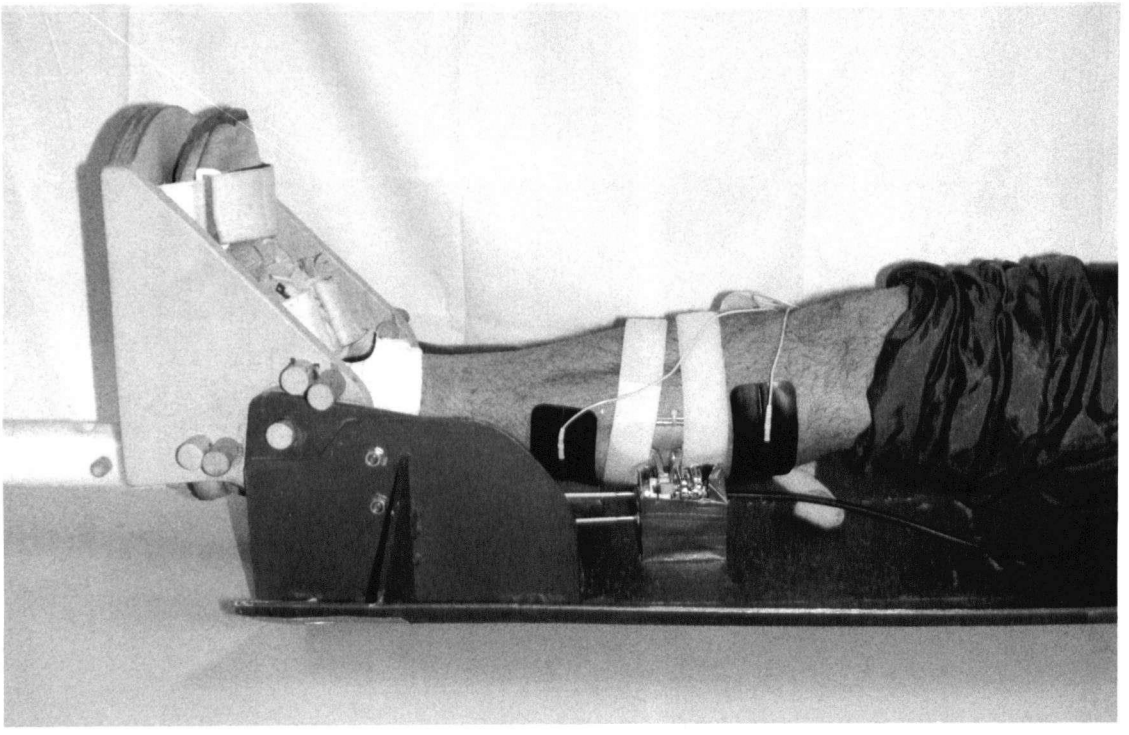

Subjects ankle was secured, in plantigrade, to the footpedal ergometer. Electrodes and RF coil are fixed to the medial gastrocnemius muscle

Figure 3
Glass Fiber Rod Attachment to Footpedal Ergometer

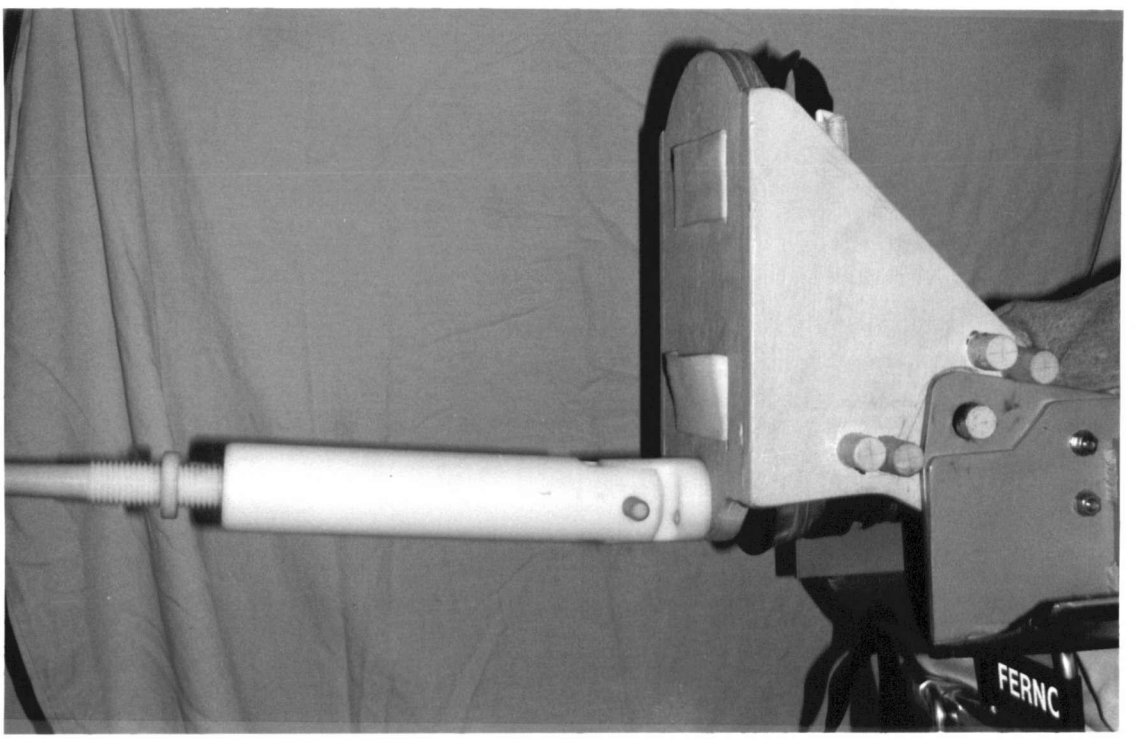

The glass fiber rod was attached to the bottom of the footpedal inferior to the axis of ankle motion. Preload tension was applied by the course thread at the left of the nylon attachment

2.3 Nuclear Magnetic Resonance Spectroscopy

Spectroscopic data was collected using a 1.5 tesla Phillips Gyroscan NMR unit with a 1.0 metre bore. The surface coil utilized was constructed with an interior diameter of 2 centimetres by 7.5 centimetres, and interrogated a 15 cc hemispherical volume of tissue, to a maximum depth of 2.0 cm, directly beneath the placement site. The coil was placed longitudinally between the two stimulating electrodes, over the medial bulk of the gastrocnemius muscle, and fixed in place with velcro straps and cling bandage. Once affixed the coil was positioned parallel to the longitudinal axis of the magnet, within the homogeneous region of the field.

The pulse program provided a 90 degree RF pulse of 0.05 millisecond duration at a frequency of 25.8576 megahertz. The repetition time was set a 1000 milliseconds. During each repetition 1024 data points were collected per sample, at a frequency of 2000 hertz. Data was acquired in 10 second intervals, with each resulting spectra representing the average metabolic state for that time period. Since standard concentrations of phosphorus metabolites were not utilized, only relative concentrations could be obtained from the data.

Prior to data collection the pulse program was connected to an audible buzzer within the body chamber. During data collection this buzzer sounded every 10 seconds, and served as the cue for the onset of stimulation.

Spectra obtained during data collection were processed on a ramtek workstation interfaced with a vax (digital) computer. Concentrations

obtained from spectral peak areas were multiplied by the following relaxation constants prior to data collection; i) Pi/PCr x 1.27, ii) βATP/PCr+Pi x 0.328.

Relative change in intracellular pH was calculated on the basis of the chemical shift difference between the centre of Pi and PCr peaks on the NMR spectrum [74]. This value is used to determine the average relative cellular pH in the tissue under investigation, with an accuracy of 0.05 pH units [73]. pH values were obtained form chemical shifts using the following formula:

$$pH=pK-\log\ (\delta obs-\delta HPO_4^{-2})/(\delta H_2PO_4^{-}-\delta obs)$$

where δobs is the observed Pi chemical shift, and pK is 6.80. $-\delta HPO_4^{-2}$ and $\delta H_2PO_4^{-}$ represent the chemical shifts at very basic (pH=10) and acidic (pH=4) pH values. For the pH calculations in this investigation it was assumed that $-\delta HPO_4^{-2}$ = 3.19 ppm and $\delta H_2PO_4^{-}$ = 5.72 ppm.

2.4 Force Measurements

Within the NMR body chamber plantar flexor force measurements were obtained using a non magnetic foot pedal ergometer coupled to a load cell by a 1.5 metre glass fiber rod (figure 2) Following application of the RF uptake coil and EMS electrodes subjects were positioned supine on the NMR body tray. The dominant foot was placed on the foot pedal,with care taken to align the ankle joint axis (inferior aspect of medial malleoli) with the foot pedal axis. The foot, calf, and knee were then stabilized with velcro straps.

Once the subject was firmly and comfortable attached to the foot pedal ergometer the calf was positioned in the centre of the magnetic

field within the NMR body chamber. A nonmagnetic Glass fiber rod, 1.5 cm in diameter was attached to the inferior surface of the foot pedal below the ankle joint axis, via a nylon pin (figure 3). Thus isometric plantar flexion of the ankle produced forefoot pressure (directed inferiorly) on the pedal above the pedal axis. This in turn produced a tension force on the glass fiber rod (attached below the pedal axis)(figure 4). The rod was then directed through a small hole in the copper screen at the foot end of the magnet. A nylon roller, on a wooden support stand, was then placed in the middle of the rod to insure that it remained parallel to the body tray throughout its length. Adjustments in the length of the rod were made via a 15cm course nylon thread at the pedal end of the rod (figure 3).

An aluminum load cell* was attached to the wall 1.5 metres from the foot end of the magnet and attached to the glass fiber rod by a nonmagnetic bolt. Prior to data collection the load cell was calibrated in tension inside, and outside, the magnetic field using a series of certified weights¶ . A ten metre cable connected to the load cell to a 12 bit data acquisition card§ installed in a Macintosh SE microcomputer. This instrumentation enabled continuous (two samples per second) acquisition of tension data with an accuracy of +/- 0.05 Newtons. Force production was calculated from data collected in the middle eight seconds of each contraction. z Omitting the first and last seconds of force data from these calculations eliminated the effects of force decline associated with the 0.5 second current rise and fall at the start and end of each protocol.

---

* Interphase Inc., Phoenix, AZ.

¶ Lumex Inc., Ronkonkomma, N.Y.

§ Strawberry Tree Computers, Sunneyvale CA.

Figure 4
Force Acquisition Appratus

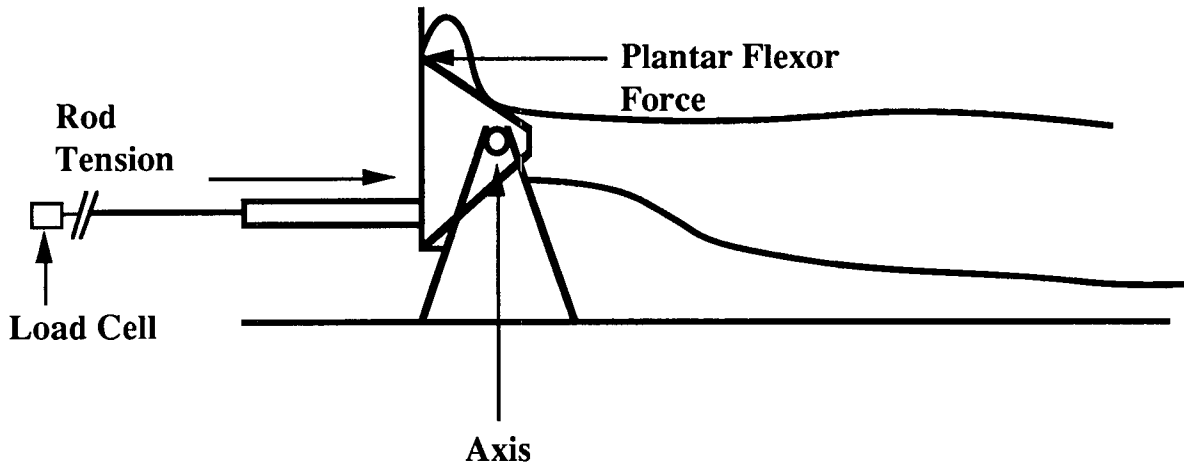

Foot is secured to the footpedal with the talocrural joint axis alligned with the footpedal axis. During stimulation Plantar flexor force is applied to the footpedal through the forefoot. This in turn produces tension on the glass fibre rod which is positioned posterior the ankle joint axis

2.5 Experimental Protocol

Following adjustment of the subjects foot on the ergometer the wire leads from the stimulator electrodes were connected to the Respond II which was fixed to the Pedal ergometer, near the subjects head. In addition a remote on/off hand switch was connected to the stimulator and fixed to the ergometer within reach of the subject. Once inside the magnet the glass fiber rod was connected to the load cell and the foot maintained in plantigrade by application of a 70 newton preload to the rod.

Each subject performed two sets of 12, 10 second EMS induced contractions. Protocol A contained ten second inter-contraction rest

periods, while protocol B contained 50 second inter-contraction rest periods.

After shimming of the RF coil, the subject was instructed to lay still to permit a resting scan of the muscle. Once the scan is taken, the protocol was as follows:

(i) two 10 second trial contractions to determine the subjects maximal current tolerance

(ii) ten minute rest

(iii) one 10 second maximal EMS contraction of the plantar flexors

(iv) rest period

(v) steps iii and iv are repeated eleven times

(vi) one hour rest period.

Subsequently, the second protocol was applied in an identical fashion. The intensity of the stimulation was very similar to the pretest levels for each subject, and was maintained at the same level throughout both protocols. The subjects manipulated the on/off switch on the stimulator in accordance with an audible buzzer wired to the NMR pulse program.

2.6 Data Analysis

NMR spectra were averaged for each 10 second period during contraction and rest during each protocol. After Fourier transformation the relative concentrations of PCr, Pi, ATP and pH were calculated on a Ramtek work station linked to a Vax (digital) computer. The areas under the appropriate resonance peaks (figure 21) were calculated, and multiplied by the appropriate relaxation constants. Relative changes in phosphocreatine were expressed as Pi/PCr, while [ATP] was expressed as βATP/PCr+Pi. Relative pH changes were calculated as described above. Changes in muscular force production during each stimulation, along with peak force output was calculated from the data recorded in the microcomputer attached to the load cell.

Statistical evaluation consisted of a repeated measures analysis of variance (ANOVA) conducted on the dependent variables (pH, ATP, force, and Pi/PCr) during each work and rest period. Specifically, tension during each 10 second contraction was compared with Pi/PCr, ATP, and pH for both protocols.

RESULTS

3.1 Stimulation

During data collection the discomfort associated with high intensity EMS produced intermittent voluntary contractions in one of the six subjects, during both protocols. Inspection of this subjects force production data revealed spontaneous and dramatic increases in muscular force output at a number of points in both protocols. Since these force measurements were consistently two standard deviations from the sample (n=5) mean this subject was classified as an outlier [93] and his data eliminated from the sample. Thus, all data presented here represents the mean values of five subjects.

Numerical data of all dependant variable collected during stimulation is presented during table 1. Means (n=5) represent the mean relative force and average observed metabolite level during each 10 second acquisition.

TABLE 1 - STIMULATION PROTOCOL A & B

Stimulation	1	2	3	4	5	6	7	8	9	10	11	12
%Force Pro A Mean/S.D.	.965/ .03	.907/ .03	.880/ .30	.829/ .10	.790/ .10	.772/ .07	.742/ .07	.738/ .07	.723/ .07	.702/ .06	.699/ .07	.672/ .07
%Force Pro B Mean/S.D.	.968/ .03	.944/ .05	.908/ .08	.878/ .10	.867/ .10	.860/ .09	.873/ .07	.857/ .07	.837/ .06	.830/ .06	.844/ .09	.842/ .07
Pi/PCr Pro A Mean/S.D.	.525/ .31	.792/ .20	1.117 /.25	1.240 /.53	1.463 /.75	1.630 /.94	1.416 /.60	1.540 /1.12	1.345 /.74	1.340 /.90	1.17/ .65	1.54/ .90
Pi/PCr Pro B Mean/S.D.	.701/ .13	.698/ .20	.914/ .36	.795/ .29	1.044 /.56	.801/ .34	.883/ .20	.850/ .17	.740/ .16	.929/ .49	.944/ .58	.875/ .41
pHi Pro A Mean/S.D.	7.151 /.05	7.100 /.06	7.055 /.05	7.042 /.05	6.970 /.10	7.010 /.14	6.940 /.15	6.904 /.12	6.914 /.14	6.902 /.16	6.850 /.16	6.850 /.16
pHi Pro B Mean/S.D.	7.150 /.05	7.100 /.09	7.060 /.06	7.040 /.08	7.070 /.05	7.030 /.12	7.050 /.11	7.060 /.12	7.060 /.01	7.070 /.07	7.060 /.10	7.070 /.09
ATP Pro A Mean/S.D.	.162/ .08	.157/ .02	.192/ .04	.155/ .04	.164/ .03	.147/ .04	.143/ .03	.171/ .08	.174/ .10	.152/ .02	.141/ .04	.171/ .04
ATP Pro B Mean/S.D.	.123/ .06	.153/ .02	.160/ .03	.150/ .02	.130/ .02	.144/ .06	.168/ .05	.139/ .04	.192/ .10	.167/ .04	.238/ .16	.153/ .03

Pro A = Protocol A (10 sec. stim./10 sec. rest.), Pro B = Protocol B (10 sec. stim./50 sec. rest.)

% Force = Average isometric force (newtons) in middle 8 seconds of each 10 second stimulation divided by the maximal force produced in that protocol.

3.1.1 Force Production

Changes in mean isometric force (newtons) were observed during each 10 second stimulation and over the course of 12 stimulations. Relative changes during each individual stimulation (figure 5) were calculated by subtracting the force output at second 2 of each stimulation, by the force output at second 9 of each stimulation. Protocol B produced negative delta values during each stimulation, indicating that force output near the end of each stimulation always exceeded force output at the onset of each stimulation. In contrast, Protocol A produced negative delta values for the first 4 stimulations, followed by progressively larger delta values for the remainder of the protocol. This indicates that during stimulation 5-12, there was a progressive increase in the force decline during each 10 second contraction. The difference in force output changes between Protocol A and B produced a significant ANOVA interaction effect ($p<0.05$).

Alterations in mean muscular force production during both stimulation protocols in illustrated in figure 6. Relative force output (y axis) represents the average EMS induced force output (newtons) in the middle 8 seconds of each 10 second stimulation, divided by the maximal instantaneous EMS induced force output in that protocol. Stimulation numbers (1-12) are shown on the x axis.

Figure 5

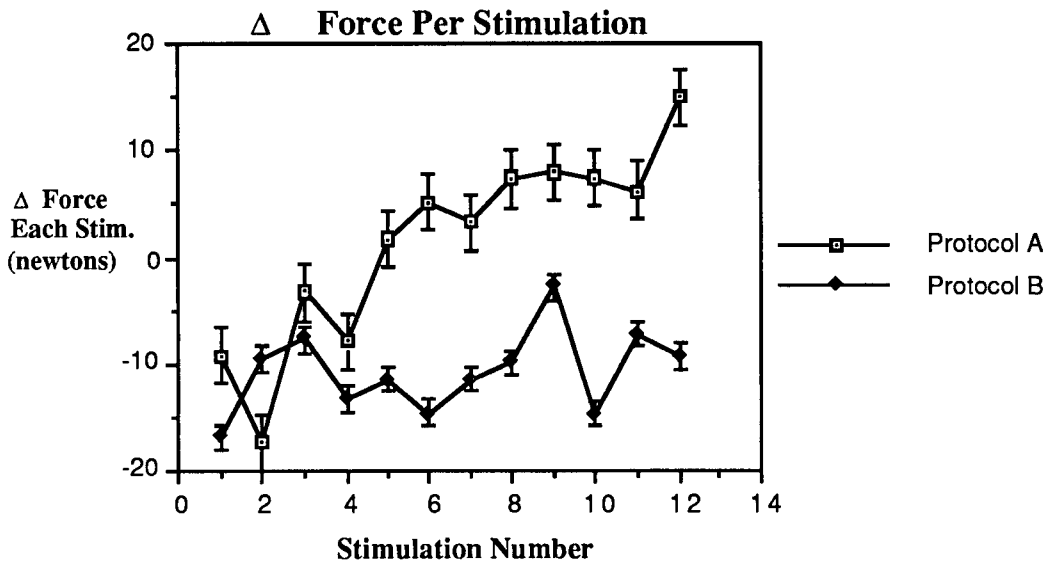

Mean change in Force (newtons) between (sec. 2-sec. 9) the second and ninth second of each stimulation in Protocol A & B

Figure 6

Force production during Stimulation

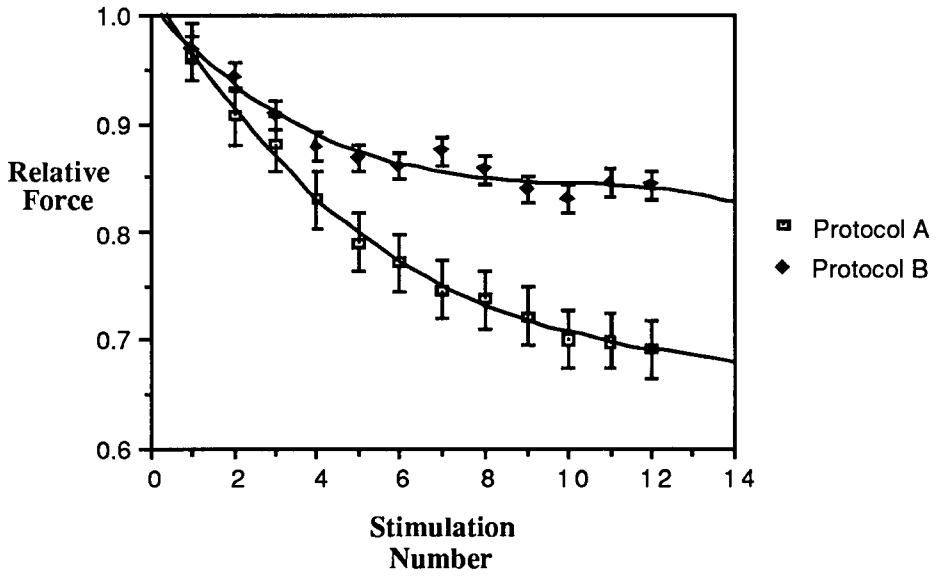

Change in relative force (newtons) over 12 x10 sec. repetitions. Protocol A = 10 sec. stimulation/10 sec. rest where y=1.03 - 6.5e-2x + 4.4e-3x - 1.1e-4x. Protocol B= 10 seconds stimulation /50 sec. rest where y=1.01 - 4.6e-2x + 4.3-3x

Over the course of 12 repetitions both protocols produced a significant decline in muscular force output ($P<0.001$). However, protocol A (ten second rest period) produced a 30% drop in force production, compared to a 13% decline in force in protocol B following 12 repetitions. Although the rest period main effect was not significant at the 0.05 level ($P=0.057$), the AB interaction (protocol x repeated force measures) was highly significant ($P<0.001$). This indicates that the changes in force production over the course of 12 repetitions differed significantly between the two protocols.

Examination of changes in force output in the time domain provides a different perspective on the relationship between force output changes during these two protocols, compared to output changes as related to stimulation number. Stimulation of the muscle during the twelfth repetition of protocol A (10 sec. on/10 sec. rest) was initiated 210 seconds after the start of the first repetition, while the onset of stimulation 12 in protocol B (10 sec. on/50 sec. rest) was initiated 650 seconds after the first repetition. Figure 7 illustrates the alterations in EMS induced force output relative to normalized time values, with 1.0 representing the end of stimulation 12 in protocol B, 660 seconds after the start of the first stimulation. The high correlation between the second degree polynomial equation and force changes during Protocol A illustrates the biphasic nature of the rapid force decline during this protocol. Force declined in a linear fashion until the seventh (t=120 sec.) repetition, when the rate of decline slowed. In contrast, the greatest rate of force decline occurred during the first four repetitions (t=180 sec) in Protocol B

Figure 7
Force Production vs Relative Time

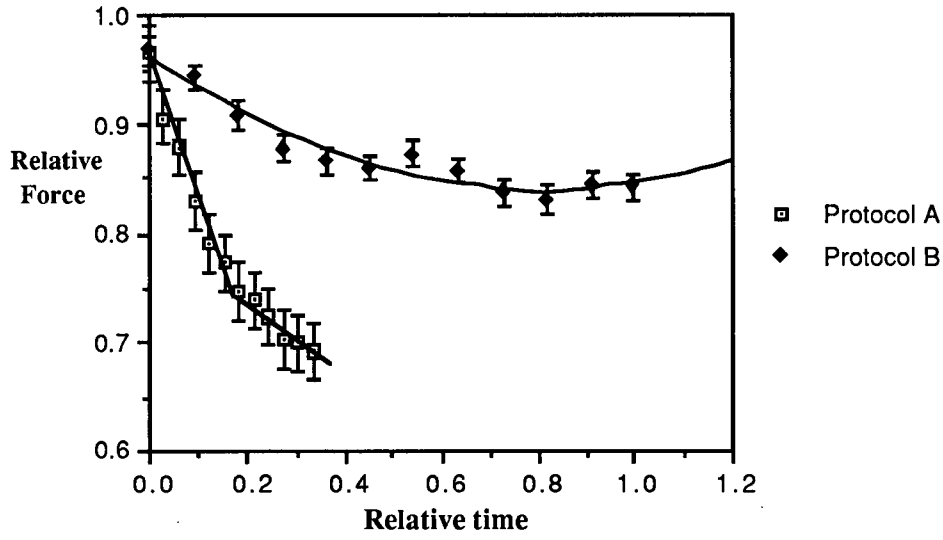

Force data presented over relative time where 1.0=660 seconds. Protocol A=10 sec. stim/10 sec. rest where y=.96-1.6x + 2.5x2. Protocol B=10 sec stim/50 sec rest where y=.97-.30x + .20x2

3.1.2 Inorganic Phosphate/Phosphocreatine

In NMR investigations, Pi/PCr is commonly used as an indicator of the amount of intracellular PCr available for ATP hydrolysis [89]. During muscle contraction an increase in the level of inorganic phosphate produced by PCr breakdown increases the numerator of this fraction, resulting in an increase in the Pi/PCr value. The significant changes ($P<0.01$) in Pi/PCr during stimulation are illustrated in figure 8. The first 10 seconds of stimulation produced a 13% and 21% increase (from resting values) in Pi/PCr level during protocol A and B respectively. In general terms protocol A produced a sharp rise in Pi/PCr levels, followed by a moderate decline in the second half of the protocol. In contrast, protocol B produced an inconsistent undulating pattern of Pi/PCr changes without a significant net change.

Figure 8
[Pi]/[PCr] Stimulation

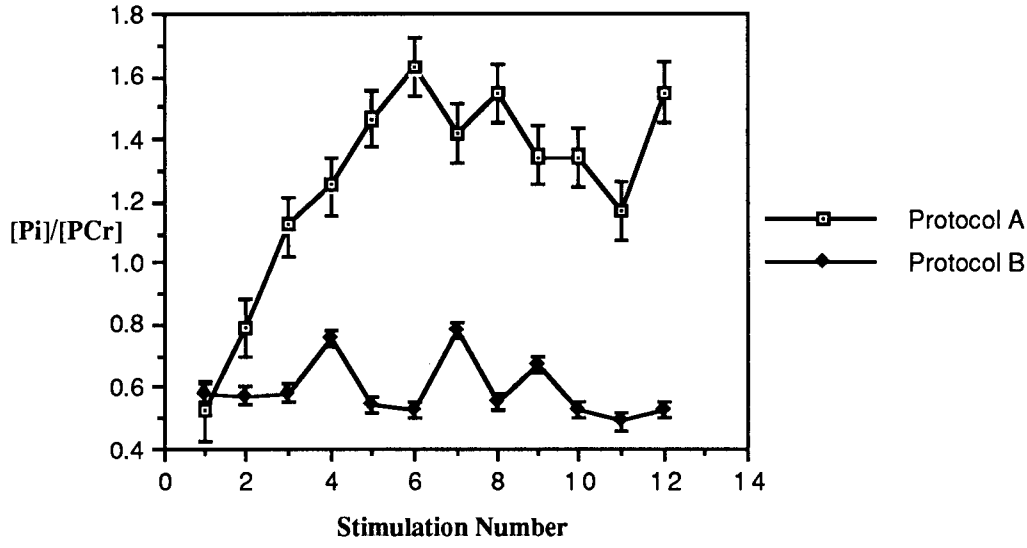

Mean (n=5) changes in [Pi]/[PCr] over 12 (10 sec.) repetitions. Protocol A (10 sec stim/10 sec. rest) produced a 210% peak increase at repetition 6, while protocol B (10 sec. stim/50 sec. rest) produced a 48% peak increase at repetition 7.

Figure 9
[Pi]/[PC] Stimulation vs Relative Time

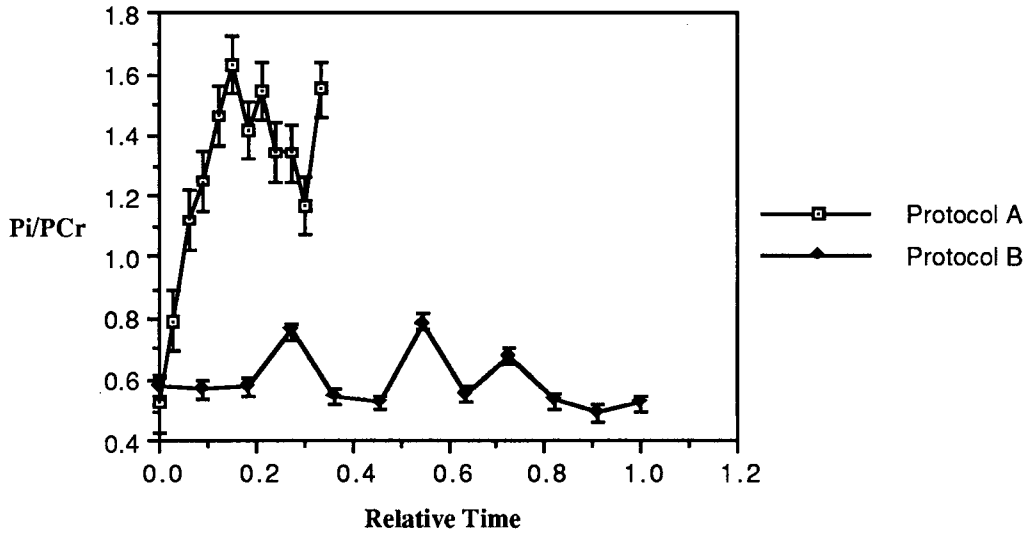

Mean changes in [Pi]/[PCr] over relative time, where 0.3 = 220 seconds and 1.0 = 660 seconds

Protocol A produced a 210% increase in Pi/PCr during the first 6 repetitions, with the greatest increase (48%) in Protocol B occurring during the seventh repetition. Following the seventh stimulation in protocol A Pi/PCr declined sharply to 122% above resting values in stimulation 11. The sharp increase in Pi/PCr between the eleventh and twelfth repetitions on protocol A resulted from a disproportionately high value in one of the data sets. This difference in the magnitude and pattern of Pi/PCr change between the two protocols resulted in a significant repeated measures and interaction effects ($P<0.05$).

Figure 9 shows the changes in Pi/PCr in relation to normalized time values. The sharp rise, and subsequent fall of Pi/PCr during protocol A, as compared to the small changes in protocol B are illustrated.

3.1.3 pHi

Initial resting scans showed equal mean resting pH values (7.11 ± 0.01) before both protocols. The significant changes in intracellular pH during both stimulation protocols are illustrated in figure 10. Initially, stimulation produced a transient cellular alkalosis. This initial alkalosis was followed by a linear drop in pH during both protocols until the fourth stimulation. Following the fourth stimulation the rapid linear drop in pH continued in protocol A, while protocol B was characterized by a shift to a gradual rise in pH during the last 8 stimulations. Thus, the statistical main effect was insignificant ($P>0.10$) with a significant repeated measures and interaction effects ($P<0.001$). In protocol A pH declined to 6.85 during the 12th stimulation, while protocol B produced a maximal pH decline to 7.04 during the fourth stimulation. Figure 11

illustrates changes in intracellular pH over relative time values. The rapid and linear drop in pH produced by protocol A is illustrated.

During protocol A changes in force output and pH_i were highly correlated(R^2=0.976), as illustrated in figure 12. In contrast, analysis of these two variables in protocol B revealed only a poor correlation(R^2=0.49/Figure 13).

Figure 10
pH Stimulation Protocol A & B

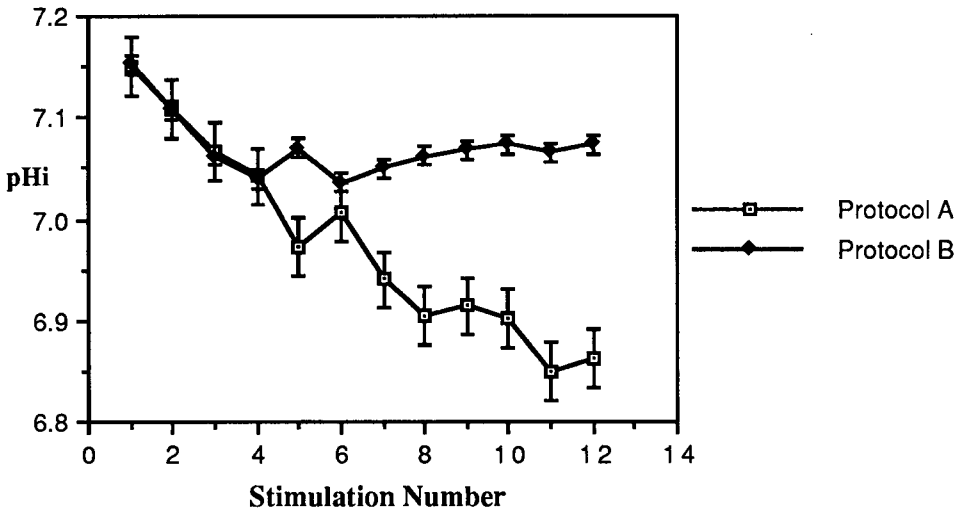

Mean pH change during each 10 second data acquisition in both protocols. Mean resting pH = 7.1

Figure 11
pH Stimulation vs Relative Time

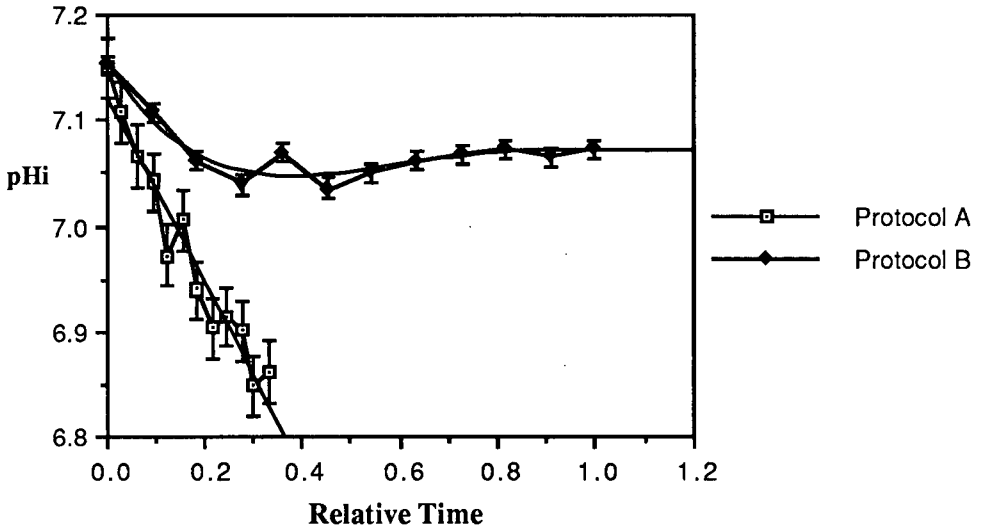

Mean change in intracellular pH during each 10 second data acquisition in both protocols. Data plotted over relative time where; 1.0=660 seconds

Figure 12
pH+Force Stimulation Protocol A

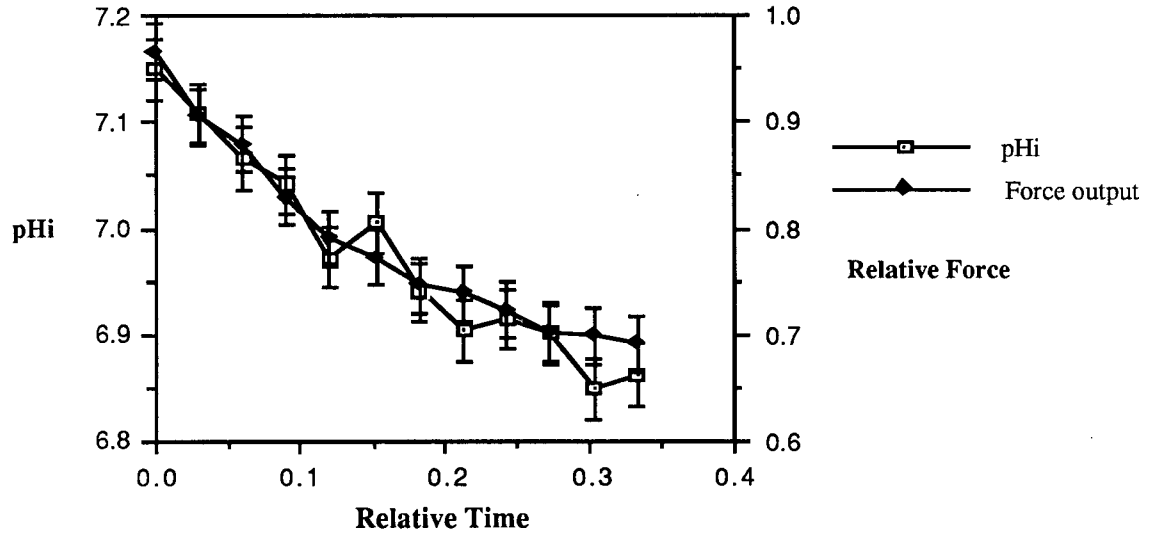

Changes in relative force production over 12 stimulations was closley correlated with changes in pHi (R=.98). Data is presented over relative time where: 1.0=660 seconds.

Figure 13
Force+pHi Stimulation Protocol B

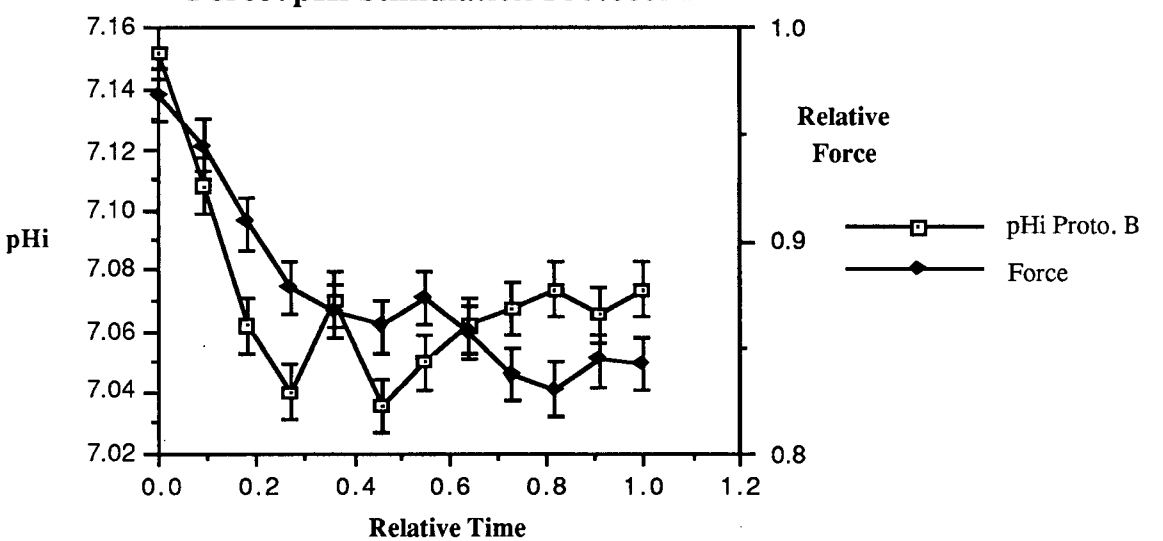

Force (newtons) and pHi during stimulation in Protocol B. Changes in Force Output were poorly correlated with pHi changes (R=.49)

3.1.4 Adenosine Triphosphate

No significant changes ($P>0.10$) were noted in relative intracellular ATP concentrations during stimulation, rest, or recovery during protocol A or B.

3.2 Rest Period Effects

Since NMR data was acquired and averaged over individual ten second periods, rest periods between contractions will be described in terms of numbers of ten second data acquisitions between each contraction. Thus, protocol A consisted of a single ten second scan, while protocol B contained 5 scans of 10 seconds duration in each inter-contraction rest period. Table 2 contains the numerical data collected during the 10 second rest period in protocol A, and the first 10 seconds of the 50 second rest period in protocol B.

TABLE 2 - 10 SECOND REST *
PROTOCOL A & B

Stimulation	1	2	3	4	5	6	7	8	9	10	11	12
Pi/PCr Pro A Mean/S.D.	.546/ .20	.909/ .24	1.285 /.54	1.499 /.80	1.524 /.80	1.566 /.90	1.617 /.56	1.77/ .22	1.590 /0.21	1.537 /1.00	1.553 /.90	1.182 /.85
Pi/PCr Pro B Mean/S.D.	.584/ .15	.573/ .13	.552/ .20	.696/ .28	.552/ .14	.528/ .18	.785/ .67	.566/ .16	.676/ .34	.532/ .13	.474/ .10	.549/ .21
pHi Pro A Mean/S.D.	7.060 /.05	7.030 /.07	7.030 /.08	6.96/ .10	6.901 /.08	6.872 /.13	6.980 /.13	6.82/ .12	6.82/ .12	6.82/ .18	6.812 /.17	6.800 /.19
pHi Pro B Mean/S.D.	7.046 /.06	7.020 /.07	7.005 /.05	6.97/ .07	6.960 /.05	6.982 /.12	6.972 /.11	6.97/ .06	6./7/ .104	6.95/ .26	6.991 /.13	6.992 /.14
ATP Pro A Mean/S.D.	.140/ .02	.106/ .11	.164/ .06	.144/ .03	.174/ .02	.161/ .03	.169/ .05	.170/ .06	.137/ .04	.168/ .03	.143/ .03	.147/ .05
ATP Pro B Mean/S.D.	.148/ .03	.179/ .03	.152/ .03	.155/ .02	.147/ .08	.182/ .06	.171/ .07	.161/ .04	.157/ .04	.123/ .04	.127/ .03	.151/ .04

Pro A = Protocol A (10 sec. stim./10 sec. rest), Pro B = Protocol B (10 sec stim./ 50 sec. rest)

10 second rest* = first 10 second NMR scan following each stimulation in both protocols

3.2.1 Inorganic Phosphate/Phosphocreatine Ratio

Both protocols exhibited a slight apparent increase in Pi/PCr during the first ten second interval following each stimulation. Pi/PCr values during stimulation and the first ten second period following stimulation for both protocols are illustrated in figures 14 and 15. Statistical analysis of Pi/PCr levels in the first ten seconds following each stimulation produced an insignificant main (protocol) effect ($P>0.10$). However, comparison of Pi/PCr levels during the first, and fifth ten second data acquisition period in Protocol B (rest) yields a significant main effect ($P<0.05$), suggesting significant PCr recovery during each rest period in Protocol B (Figure 16). Table 3 contains the data collected during the first and fifth 10 second scans during each 50 second rest period in protocol B.

TABLE 3 - 10* & 50• SECOND REST
PROTOCOL B

Stimulation	1	2	3	4	5	6	7	8	9	10	11	12
Pi/PCr 10 Mean/S.D.	.584/ .15	.573/ .14	.552/ .20	.696/ .28	.552/ .14	.528/ .18	.785/ .67	.566/ .16	.676/ .34	.532/ .13	.474/ .10	.549/ .21
Pi/PCr 50 Mean/S.D.	.277/ .16	.472/ .28	.457/ .20	.563/ .42	.379/ .33	.486/ .291	.444/ .37	.586/ .39	.501/ .34	.371/ .13	.417/ .45	.399/ .31
pHi 10 Mean/S.D.	7.046 /.06	7.021 /.07	7.005 /.05	6.972 /.07	6.963 /.05	6.982 /.12	6.972 /.11	6.970 /.06	6.970 /.10	6.952 /.26	6.991 /.13	6.991 /.14
pHi 50 Mean/S.D.	6.901 /.38	6.992 /.11	6.953 /.08	6.950 /.09	6.95/ .17	6.922 /.09	6.921 /.10	6.738 /.14	6.922 /.19	6.990 /.21	6.882 /.17	6.872 /.16
ATP 10 Mean/S.D.	.148/ .03	.179/ .03	.152/ .03	.155/ .02	.147/ .08	.182/ .06	.171/ .07	.161/ .04	.157/ .04	.123/ .02	.127/ .03	.151/ .04
ATP 50 Mean/S.D.	.159/ .05	.156/ .05	.171/ .06	.134/ .02	.137/ .023	.193/ .07	.193/ .08	.155/ .01	.135/ .02	.179/ .05	.120/ .02	.143/ .02

Pro A = Protocol A (10 sec. stim./10 sec. rest), Pro B = Protocol B (10 sec. stim./50 sec. rest)

* first 10 second resting scan following stimulation, • resting scan 50 seconds following stimulation

Figure 14

[Pi]/[PCr] Protocol A 10 Sec. Rest

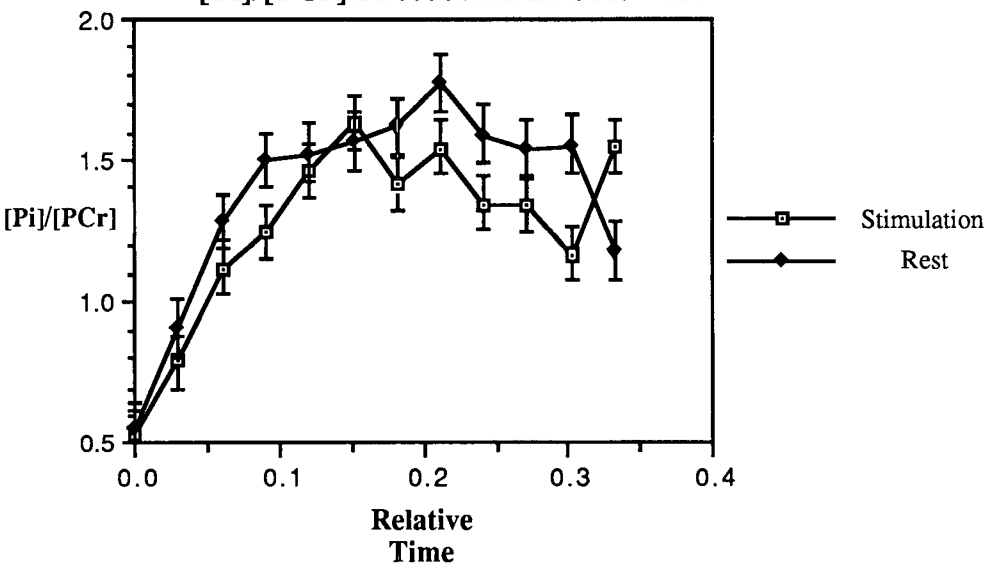

Changes in [Pi]/[PCr] during 10 second intercontraction rest periods in Protocol A

Figure 15

[Pi]/[PCr] First 10 Sec. of Rest: Protocol B

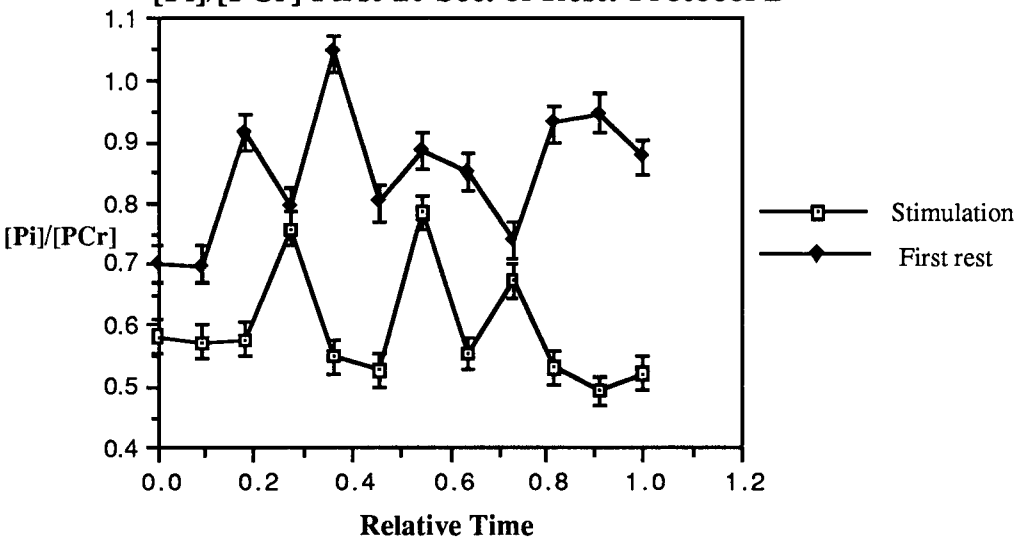

Changes in [Pi]/[PCr] during the first 10 sec. data acquistition during each 50 second rest period in Protocol B

Figure 16

1+5 10 sec. Acquisition Protocol B Rest

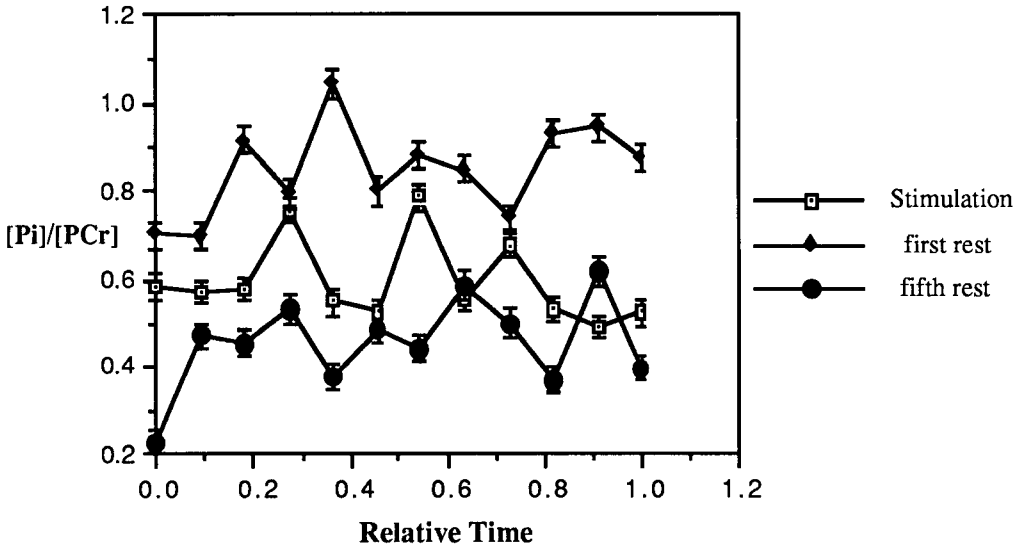

Change in [Pi]/[PCr] during the first and fifth 10 second data data acquisition during each 50 second rest period in Protocol B.

3.2.2 pH

Intracellular pH appeared to continue to decline during each ten second inter-contraction rest period in protocol A (Figure 17). However differences between the mean values over the course of protocol A were insignificant ($P<0.10$).

Figure 17
pHi Protocol A Stim & Rest

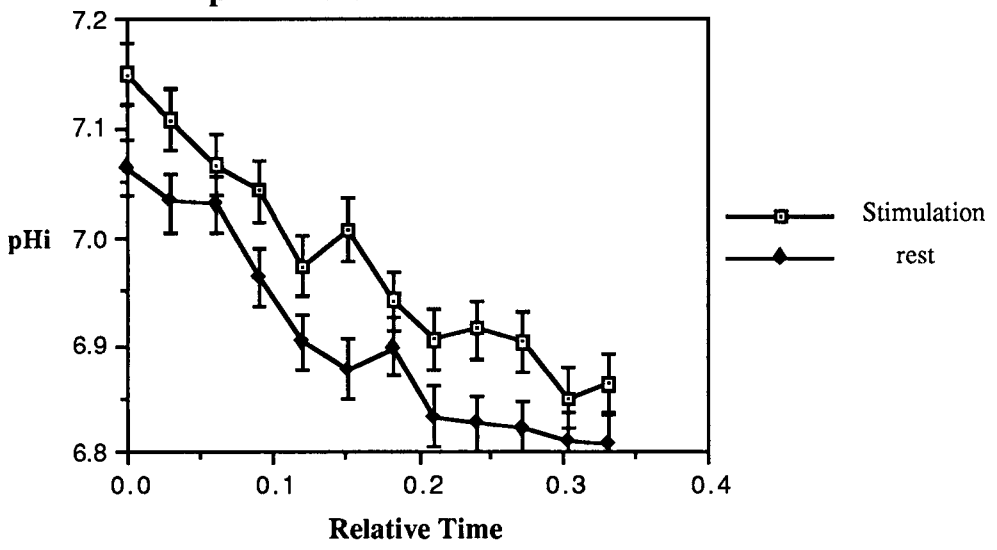

pHi changes during stimulation and 10 second rest period in Protocol A. Data is presented over relative time where: 0.34=220 seconds.

Figure 18
Protocol B 1+5 10 sec. Rest

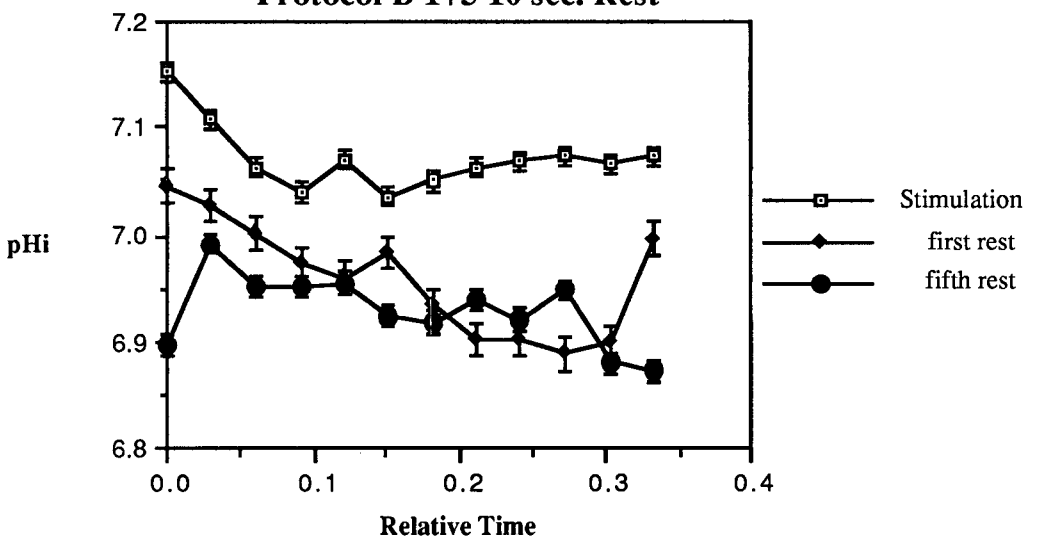

Change in pHi during stimulation, the first and fifth 10 second data data acquisition during each 50 second rest period in Protocol B.

Protocol B produced a greater, but insignificant (P>0.10), decline in pHi during the first ten seconds of each rest period (figure 18).

In addition figure 18 shows the decline in pH_i during each 50 second inter-contraction rest period in the first half of protocol B. However, slight increases in pHi can be seen between contractions 9 and 12. Despite these observed differences, the means of these three variables were not statistically different (P>0.10).

3.3 Recovery

Numerical data for [Pi/PCr], pHi, and [ATP] is presented in Table 4.

3.3.1 Inorganic Phosphate/Phosphocreatine Ratio

Following twelve stimulations ten seconds NMR scans were collected for 90 minutes. A drop in inorganic phosphate signal below resting levels following intense muscle contraction has previously been observed [4]. Unfortunately, this drop in Pi peak after two minutes made it impossible to follow Pi/PCr or pH changes beyond 100 seconds. Thus, recovery scans are only reported for 100 seconds post stimulation.

Pi/PCr values exhibited a rapid drop to resting levels within 100 seconds following both protocols (figure 19)

3.3.2 pH

In contrast pHi values continued to decline for 90 seconds following both protocols (figure 20). However, pHi began a sharp increase 100 seconds following the end of the last stimulation bout in both protocols.

TABLE 4 - RECOVERY

Seconds x10	1	2	3	4	5	6	7	8	9	10
Pi/PCr Pro A Mean/S.D.	1.420 /.62	1.110 /.67	.860/ .47	.690/ .44	.734/ .41	.489/ .29	.537/ .33	.555/ .43	.381/ .19	.667/ .21
Pi/PCr Pro B Mean/S.D.	.761/ .53	.474/ .46	.285/ .22	.560/ .68	.536/ .48	.446/ .46	.293/ .12	.286/ .19	.241/ .07	.199/ .05
pHi Pro A Mean/S.D.	6.772 /.20	6.770 /.22	6.762 /.21	6.791 /.30	6.763 /.29	6.740 /.20	6.321 /.32	6.722 /.26	6.692 /.29	6.700 / .32
pHi Pro B Mean/S.D.	7.061 /.09	6.984 /.13	6.763 /.11	6.952 /.11	6.923 /.25	6.890 /.21	6.870 /.19	6.890 /.23	6.821 /.25	6.821 /.12
ATP Pro A Mean/S.D.	.165/ .04	.150/ .05	.142/ .03	.143/ .03	.130/ .040	.152/ .07	.152/ .04	.155/ .03	.152/ .02	.159/ .08
ATP Pro B Mean/S.D.	.178/ .20	.153/ .04	.165/ .07	.163/ .06	.276/ .33	.154/ .04	.116/ .01	.118/ .03	.129/ .07	.163/ .15

Pro A = Protocol A (10 sec. stim./10 sec rest)
Pro B = Protocol B (10 sec stim/50 rest)

Figure 19

Pi/PCr 100 Sec. Recovery

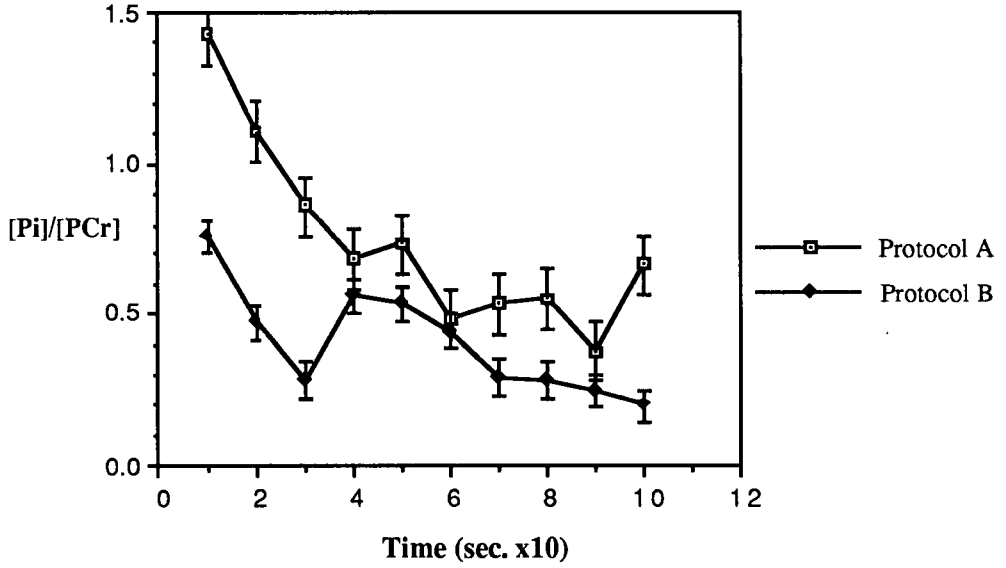

Changes in Pi/PCr following 12, 10 second tetanic stimulations in both protocols.Data presented for10x10 second data acquisitions.

Figure 20

pH 110 Sec. Recovery

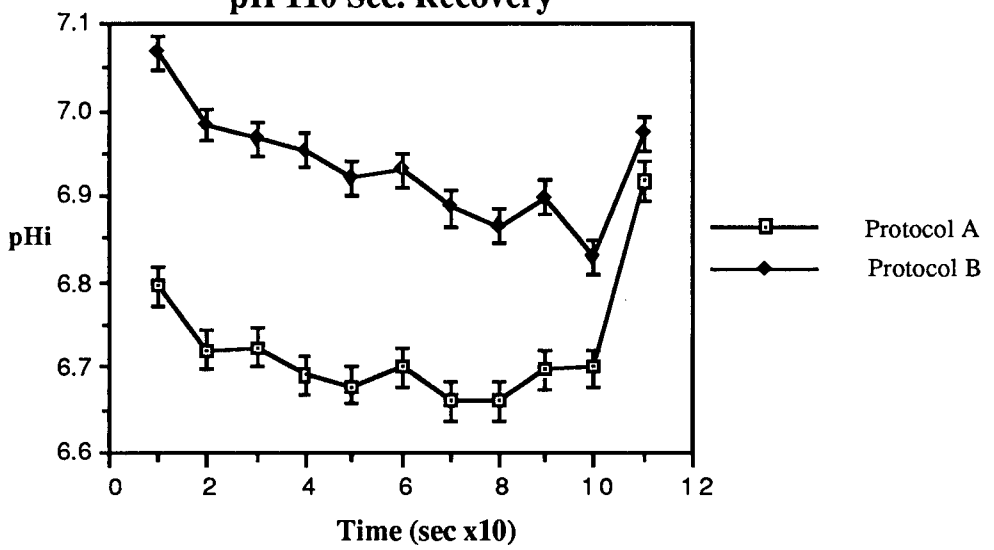

Changes in pHi during 11, 10 second data acquisitions following both stimulation protocols.

DISCUSSION

Electrical muscle stimulation delivered using surface electrodes produced a localized tetanic contraction resulting in initial external force production equal to 40-45% of MVC. Both stimulation protocols utilized in this investigation contained equal total stimulation time and were conducted at identical current intensities. Thus, only events occurring during the inter-contraction rest periods could have been responsible for variations in the mechanical and metabolic response between the two protocols.

4.1 Protocol A

In general Protocol A produced greater changes in force production, Pi/PCr concentration, and intracellular pH than protocol B (figure 21). During stimulation protocol A produced a rapid initial decline in force output, followed by a reduction in the rate of force decline after the seventh stimulation (figure 7). The magnitude of force decline between the first and twelfth repetition (30%), is in close agreement with the 26% decline observed by Cox et al [24] following 10 EMS induced contraction with a 1:3 work/rest ratio. During stimulations 1-4 force production continued to increase between the start and end of each 10 second stimulation (as illustrated by the negative delta values in figure 5). The increase in delta values between stimulations 5 and 12 suggest a progressive inability to maintain force during each contraction, as reflected in changes in mean force production over the same period.

Figure 21
Σ Delta Values - Stimulation Protocol A & B

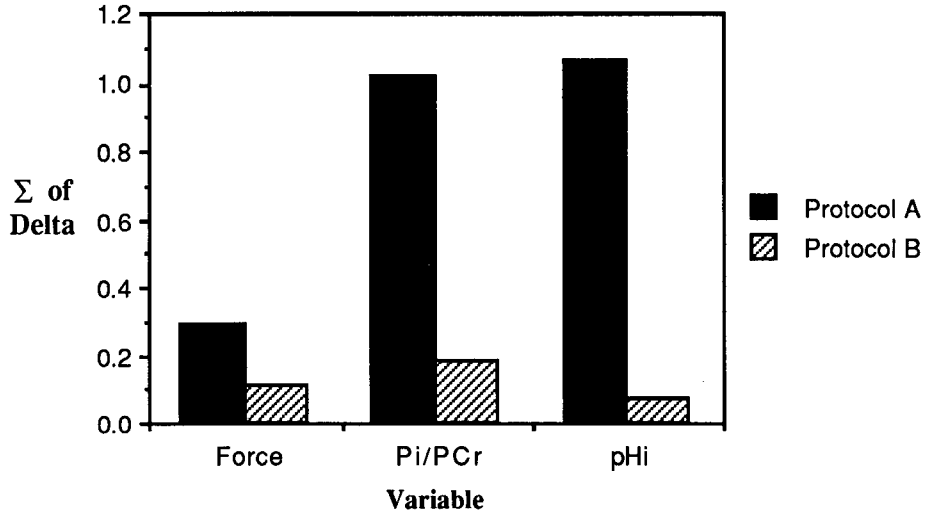

Sum of individual delta values during stimulation.(stim1- stim 2.+ stim 2-stim 3+... stim 11- stim 12)

The early decline in force output was accompanied by a rise in Pi/PCr levels during the first six stimulations of protocol A (figure 9). The 210% increase in Pi/PCr values is similar to the PCr changes reported by Shenton [94] following a similar investigation of the response of the forearm flexors to EMS. Following the sixth stimulation, Pi/PCr levels returned to 189% above resting levels by the eleventh stimulation. Interestingly, the onset of decline in Pi/PCr coincided with the onset of reduction in force decline in protocol A. Hultman [48] observed a close relationship between PCr concentration and EMS induced force production in muscle with occluded circulation. However, he found this relationship to be less obvious when circulation was intact.

Subjects exhibited the same mean resting intracellular pH values (7.11) before stimulation in both protocols. Although this value is higher than normal resting values obtained by microelectrodes (pH=7.0) [66],

they are in close agreement with resting values reported several NMR studies of resting human muscle, and is thought to represent an accurate cytoplasmic pH [20, 68, 94, 95].

Initial cellular alkalosis was produced by proton uptake secondary to PCr breakdown [4]. Following this rise in pH, intracellular pH exhibited a rapid drop from the onset of protocol A.(figure 11) The activation of glycolysis within the first second of Maximal EMS was previously reported by Hultman [47]. The decline in pH_i to 6.85 is not indicative of the severe acidosis associated with maximal exhaustive exercise (decrease in pH>0.6 units [102]), but is similar to changes observed following short maximal isotonic quadriceps work [95] and intense weight training [103]. The strong correlation between pH_i and force output in protocol A (R^2=.98-figure 12) indicates a close relationship between these two variables. Although causation may not be inferred from association, a reduction in contractile force is commonly observed secondary to a reduction in pH_i during high intensity EMS [52]. However, reduction in intracellular pH in the absence of fatigue (induced by CO_2 perfusion of isolated muscle) produced significantly less force decline than exhibited during exercise induced fatigue [72, 82]. These results indicate that pH changes act in conjunction with other cellular changes during fatigue to inhibit force production.

Adenosine triphosphate depletion during exhaustive exercise has a profound effect on other cellular energetic processes [102]. However, ATP depletion does not commonly occur during maximal short duration isolated muscle work, with significant fatigue often occurring in the absence of severe ATP depletion [48, 95], In this investigation [ATP] did

not exhibit a significant changes during stimulation, rest, or recovery, in either protocol.

Metabolic recovery between contractions in protocol A was negligible. The apparent rise in Pi/PCr levels during each 10 second rest period is difficult to explain. This finding contrasts sharply with the 10% recovery of PCr observed by Shenton 8 seconds after a 10 second EMS induced contraction. Each value reported here represents the average change in Pi/PCr over each 10 second acquisition period. Thus, it is possible that Pi/PCr increases in the first few seconds following stimulation produced a net 10 second Pi/PCr increase, despite a decline in this value near the end of each rest period.

The continued decline in pH_i during each 10 second rest period indicated that the rate of lactate production exceeded the rate of clearance, resulting in an significant increase in intracellular $[H^+]$ during the short rest period. Although Pi/PCr showed a net increase between contractions, any PCr resynthesis during this period would have also increased the proton load on the cells. The insignificant differences between Pi/PCr (figure 14) and pH_i (figure 17) levels during stimulation and the subsequent rest period indicate a continuous, cumulative depletion of PCr accompanied by a decline in pH_i. These results indicate that a 1:1 work rest ratio was insufficient to allow significant metabolic recovery between 10 second contractions. This supports the observation of Duchateau [31] that EMS delivered with a 1:1 work/rest ratio (one second on/one second off) protocol produces a similar decline in force production to a single continuous stimulation. In fact, if the inter-contraction rest period is too short to allow significant metabolic

recovery, repeated contraction and relaxation may demand an even greater energy expenditure that a single continuous contraction [8].

Since the inter-contraction rest period allowed no metabolic recovery, changes in extracellular processes must have been responsible for the alteration in the pattern of force decline and Pi/PCr change observed following the sixth repetition (t=120 sec.) in Protocol A. It reasonable to speculate that the increase in Pi/PCr and slowing of the rate of force decline was a product of an increase in local blood flow.

The mechanical occlusion of capillary blood flow during isometric contractions over 30% MVC has been established [80, 90]. Considering the localized and maximal nature of electrically induced contractions, this mechanism may be even more consequential during the application of EMS. However, the relationship between blood flow and recovery between intermittent contractions has not been well described.

EMS to the human calf producing 30% MVC results in a significant increase in regional blood flow between one and two minutes following the onset of stimulation [27]. EMS applied to the human quadriceps with open and occluded circulation produced identical change in PCr, pH, and ATP, until 110 seconds after the onset of stimulation (1.6 seconds stim/1.6 seconds off). Following 110 seconds the open circulation model exhibited an increase in force output, pH, PCr, and ATP not displayed by the muscle with occluded circulation [48, 52]. The author suggested that an increase in local blood flow after 110 seconds increased the local oxygen supply, (and thus oxidative metabolism) in the contracting musculature [48, 52]. This increase in oxidative metabolism in turn produced oxidative PCr resynthesis. Considering the time frame of these

changes it seems plausible that an increase in local blood flow produced the observed alterations in the pattern of Pi/PCr utilization and force output during the second half of protocol A.

4.2 Protocol B

Over the course of 12 stimulations, protocol B produced a significantly smaller decline in force output than protocol A. Throughout the protocol force production at the end of each stimulation exceeded force production at the start of that stimulation (as illustrated by the negative delta values in Figure 5). This indicates that prior to each stimulation the muscle cell had recovered sufficiently to produce near maximal force throughout each stimulation period.

This reasoning is supported by the small (13%) decline in mean force between the first and twelfth stimulation, compared to the 30% decline observed following protocol A. The 13% decline in force production following 12 stimulations in protocol B is greater that the decline reported by Baker [6] following 30 minutes of stimulation of the peroneal muscles(1 sec stim/5 sec off) with implanted electrodes. However, the 13% force decrement is less than the 20% decline reported by Cox [24] after 10 stimulations (10 sec stim/50 sec off) of the human quadriceps. The greater torque decrement reported by Cox may have been related to the intensity of stimulation (60-88% MVC) in her investigation [24].

During the first stimulation the increase in Pi/PCr was greater in protocol B (21%) than in protocol A (13%) Thereafter, protocol B produced small, erratic changes in Pi/PCr concentrations, with no net change over the course of 12 stimulations (figure 8). The significant

($p<0.05$) drop in Pi/PCr levels between the first and fifth 10 second data acquisition during each rest period (figure 6) illustrates the magnitude of PCr recovery that occurred between contractions in protocol B.

Near full Pi/PCr recovery in 50 seconds exceeds the rate of Pi/PCr recovery (1/2 time=1.2 min.) reported following light dynamic forearm exercise [4]. High rates of aerobic metabolism within the mitochondria provided the ATP necessary to partially restore intracellular [PCr] prior to the next stimulation [20]. In turn the production of H^+ associated with PCr resynthesis contributed to the maintenance of low pH levels during each rest period (figure 18) [4].

Following transient alkalosis, the sharp initial drop in intracellular pH during protocol B (figure 10) illustrates the rapid activation of anaerobic energy sources during EMS reported by other investigators [47, 50]. However, following the fourth stimulation (t=180), pH stopped declining and increased slightly between stimulations 6 and 12. Although rapid activation of anaerobic glycolysis at the onset of stimulation with open circulation has been well described, the pH decline in the absence of significant Pi/PCr changes is perplexing.

Initial PCr breakdown acts as a proton sink, producing cellular alkalosis (as illustrated by the rise in pH values from 7.11 at rest to 7.15 following stimulation 1 in protocol B). However, PCr resynthesis during the subsequent rest period resulted in significant acidosis (figure 18) [4]. In addition to PCr hydrolysis, anaerobic glycolysis also contributed to the proton load on the cell [47]. Perhaps following stimulation 4, the cellular proton load (and pH decline) was attenuated by an increase in proton clearance, without a change in proton production.

The most rapid decline in force occurred between the first and fourth repetitions (t=180 sec.), and coincided with the highest rate of pH_i decline during this protocol. This change in the pattern of pH_i and force decline occurred about the same time similar changes occurred in protocol A (t=120 sec). As discussed previously, the alteration in the pattern of pH change following stimulation may be related to changes in peripheral blood flow [48, 52]. It seem likely that the longer rest period in protocol B would result in greater metabolic changes secondary to alterations in peripheral blood flow, than might be observed following similar blood flow changes during protocol A.

Despite the similar patterns of change observed in force production and pH during protocol B (figure 13) the correlation between the two variables was low (r=.49). This finding contrasts sharply with the high correlation (r=.90) between force and pH observed by McCully et al [69] during 1 second on/5 seconds off voluntary resisted isotonic contractions of the forearm flexors. Although the work/rest ratio was the same in both investigations, the ten fold difference in stimulation time may have contributed to the observed difference. Gentz [40] noted that large increases in contraction duration, without changes in work/rest ratio, produced a reduction in fatigue associated with EMS induced contractions. Dramatic changes in pH during stimulation 5, without associated changes in force output, may have also contributed to the low observed correlation.

4.3 Recovery

Following EMS induced contractions cellular metabolic processes began rapidly returning the cells to a resting state. During this process

resynthesis of PCr is catalyzed by creatine kinase [20]. Since this reaction is maintained near equilibrium [PCr] will be determined by concentrations of other metabolites that control the reactions equilibrium [4]. Following moderate exercise the level of intracellular acidosis is probably the major determinant of the rate of PCr resynthesis [4].

After stimulation 12 in protocol A and B the Pi/PCr level fell rapidly for 40 seconds then more gradually for the next 60 seconds. Despite the higher post stimulation Pi/PCr in protocol A, both groups exhibited a drop in Pi/PCr to below resting levels 100 seconds after stimulation 12. This phenomenon is a function of the drop in Pi below resting levels previously observed in NMR investigations of skeletal muscle [4, 102]. This rate of recovery is in close agreement with the rate observed by Arnold following moderate forearm exercise [4].

Low levels of intracellular pH following exercise or circulatory occlusion will slow PCr resynthesis [4, 102]. Evidently the 0.3 pH unit drop observed in protocol A was insufficient to impair PCr resynthesis.

Following stimulation pH_i continued to decline for 90 seconds. This poststimulation decline is a product of the increase in the proton load resulting from PCr resynthesis [4]. Similar post exercise decline, followed by an return to resting pH levels between two and eight minutes post exercise, was observed by Taylor et al [102]

One hundred seconds after the last stimulation in both protocols pH_i exhibited a a rapid increase toward resting levels. Interestingly, this abrupt change coincides with the return of Pi/PCr to near resting levels. On the basis of results of similar investigations of voluntary exercise it

has been hypothesized that the cessation of PCr resynthesis facilitates the normalization of intracellular pH values [4].

4.4 Clinical Implications

Based on the results presented here the gastrocnemius muscle responded quite differently to application protocols A and B. Protocol A produced considerable glycolytic activity, which resulted in significant reduction in muscular force production and pH over the course of 12 stimulations. The strong correlation between force output and pH in protocol A seemed to imply some association between the two variables. In contrast, protocol B provoked an small initial decline in pH and force output, followed by a 'steady state' period characterized by a lack of net change in [Pi]/[PCr] or pH. Thus, it is clear that these two protocols would provide different metabolic stimuli to skeletal muscle exposed to electrical muscle stimulation of equal duration.

The ability to extrapolate these findings to clinical practice is dependant on the relationship between the physiological state of the investigated muscle, the type of muscle and, the type of muscle work, to the rehabilitation setting. Disuse atrophy [11] and vascular insufficiency [18] inhibit force production at several sites within the neuromuscular system. Thus, the results of this investigation on the response of healthy muscle should be used only as a guideline in the application of EMS to these patient populations. Further investigation into the response of specific type of muscle dysfunction to EMS would provide direct application to clinical use of electrical muscle stimulation.

The difference in metabolic response between different muscle fiber types in well documented, and could dramatically effect the results of

this type of study [25]. Since the proportion of specific fiber types within a muscle exhibits some variability among individuals, and fiber type was not examined in these subjects, it is impossible to describe the fiber characteristics of the stimulated muscle in this study. However, investigation of the fiber composition of the gastrocnemius in 35 middle age men and women showed a equal distribution of oxidative (S.O.) and glycolytic (F.G) and intermediate (F.O.G.) muscle fibers throughout the muscle [32]. Interestingly, the fiber composition of this muscle did not appear to differ significantly from the reported fiber composition of the human vastus lateralis, a muscle commonly utilized in EMS investigations [32].

Voluntary muscle strengthening regimes commonly employ repeated contraction against a high resistance to the point of complete subjective fatigue [103]. This method is advocated in order to achieve maximal fiber recruitment, and produce maximal tension in recruited fibers. However, subject motivation [86], motor learning factors [85],substrate availability [29], vascular supply [18] , and central fatigue mechanisms [10], can all effect the response of skeletal muscle to voluntary strength training.

Peripheral activation of the muscle by EMS eliminates the effects of subject motivation, insuring the maximal (all or none) activation of all fibers within the area of current flow. Accordingly conventional rehabilitation protocols encourage the application of EMS in a manner that facilitates repeated contractions and minimizes progressive fatigue over a given number of contractions. This principle is illustrated by the mechanical response of the muscle in protocol B.

However, fatigue is a widely recognized stimulus for muscle adaptation. Severe fatigue induced by long term EMS provides a stimulus powerful enough to produce complete fiber type conversion in skeletal muscle [87] In addition, muscular "overload" induced by high intensity/short duration contractions are advocated for the development of increased muscle mass and strength in healthy individuals [5, 22] Protocol A produced significant muscle fatigue accompanied by substantial metabolic changes during 120 seconds of electrical stimulation. These mechanical and metabolic alterations are similar to those observed during high intensity voluntary training [95, 103]. Thus, if fatigue resulting from failure of the contractile apparatus is the critical stimulus for adaptation, protocol A should provide a more effective training stimulus.

CONCLUSION

This study has examined the effects of alteration in rest period length between repeated 10 second EMS induced contractions on glycolytic metabolism and muscular force production. The results suggest that: i) tetanic EMS (40 hertz) applied to human muscle results in a rapid activation of glycolysis, producing a sharp initial increase in Pi/PCr and a decrease in intracellular pH with 10 seconds of stimulation, ii) a 1:5 work/rest ratio produces an initial reduction in pH, force output, and an increase in Pi/PCr, followed by a steady state period characterized by insignificant changes in these variables, iii) a 1:1 work/rest ratio resulted in significant glycolytic activity characterized by a linear reduction in pHi strongly correlated with a near linear reduction in muscular force output throughout the protocol.

Alterations in the pattern of metabolic and force output changes during intermittent stimulation suggests that changes in peripheral blood flow influenced glycolytic metabolism during intermittent isometric EMS. These changes were observed following two to three minutes of stimulation during both protocols.

REFERENCES

1. Ahlborg, B., J. Bergstrom, L. Ekelund, G. Guarnieri, R. C. Harris, E. Hultman and L. Nordesjo. Muscle metabolism during isometric exercise performed at constant force. J. Appl. Physiol. **33**(2): 224-228, 1972.

2. Albo, S. K. NMR study of Radiation Effects on the Human Brain. 1990., Masters Thesis, University of Alberta

3. Alon, G., J. Allin and G. F. Inbar. Optimization of Pulse Duration and Pulse Charge During Transcutaneous Electrical Nerve Stimulation. Aust. J. Physiother. **29**(6): 195-201, 1983.

4. Arnold, D. L., P. M. Matthews and G. K. Radda. Metabolic Recovery after exercise and and the assessment of mitochondrial function in vivo in human skeletal muscle by means of 31p NMR. Mag. Res. Med. **1**: 307-315, 1984.

5. Atha, H. "Strengthening Muscle." Exercise Science and Sports Reviews. Miller ed. 1981 Franklin. Philadelphia.

6. Baker, L. L., L. A. Benton, B. R. Bowman and R. L. Waters. "Functional Electrical Stimulation." 1981 Rancho Los Amigos Hospital Association. Downey California.

7. Bandy, W. D., V. Lovelace and B. Mckitrick. Adaptation of Skeletal Muscle to Resistance Training. J. Orthop. Sports Phys. Ther. **12**(6): 248-255, 1990.

8. Bergstrom, M. and E. Hultman. Energy cost and fatigue during intermittent electrical stimulation of human skeletal muscle. J. Appl. Physiol. **65**(4): 1500-1505, 1988.

9. Bigland-Ritchie, B., F. Bellemare and J. J. Woods. "Excitation Frequencies and sites of Fatigue." Human Muscle Power. Jones, McComas and Mccartney ed. 1986 Human Kinetics. Champaign Illinois.

10. Bigland-Ritchie, B., D. A. Jones and J. J. Woods. Excitation Frequency and Muscle Fatigue: Electrical Response During Human Voluntray and Stimulated Contractions. Exp. Neurol. **64**: 414-427, 1979.

11. Booth, F. W. and P. D. Gollnick. Effects on disuse on the structure and function on skeletal muscle. Med. Sci. Sport and Exer. **15**(5): 415-420, 1983.

12. Brooks, G. A. Anaerobic threshold: review of the concept and directions for future research. Med. Sci Sports and Exer. **17**(1): 22-31, 1985.

13. Brooks, G. A. Lactate production under fully aerobic conditions: the lactate shuttle during rest and exercise. Fed, Proc. **45**: 2924-2929, 1986.

14. Brooks, G. A. and T. D. Fahey. "Exercise Physiology: Human Bioenergetics and Its Applications." 1984 John Wiley and Sons. New York.

15. Burt, C. T., J. Koutcher, J. T. Roberts, R. E. London and B. Chance. Magnetic Resonance Spectroscopy of the Musculoskeletal System. Radio. Clin. North. Am. **24**(2): 321-331, 1986.

16. Cabric, M., H. J. Appell and A. Resic. Effects of Electrical Stimulation of Different Frequencies on the Mononuclei and Fiber size in Human Muscles. Int. J. Sports Med. **8**: 323-326, 1987.

17. Cabric, M., H. J. Appell and A. Resic. Fine structural changes in electrostimulated human skeletal muscle. Eur. J. Appl. Physiol. **57**: 1-5, 1988.

18. Challiss, R. A., D. J. Hayes, R. F. Petty and G. K. Radda. An investigation of arterial infufficiency in rat hindlimb. Biochem J. **236**: 4611-467, 1986.

19. Chance, B., S. Eleff and J. S. Leigh. Noninvasive, Nondestructive Approches to Cell Bioenergetics. Proc. Nat. Acad. Sci. **77**(12): 7430-7434, 1980.

20. Chance, B., A. Sapega, D. Sokolow, S. Eleff, J. S. Leigh, T. Graham, J. Armstrong and R. Warnell. "Fatigue in Retrospect and Prospect: 31P NMR Studies of Exercise Performance." Studies of Exercise Performance. Knuttgen, Vogel and Poortmans ed. 1983 Human Kinetics. Champaign, Il.

21. Chokroverty, S. Hemiplegic Amyotrophy. Arch. Neurol. **33**(Feb.): 104-110, 1976.

22. Clarke, D. Adaptations in Strength and Muscular Endurance Resulting from Exercise. Exer. Sci. .Sports .Rev. **1**: 73-102, 1973.

23. Cote, C., J. A. Simoneau, P. Lagasse, M. Boulay, M. Thibault and C. Bouchard. Isokinetic Strength Training Protocols, Do They Induce Skeletal Muscle Fiber Hypertrophy? Arch Phys. Med. Rehabil. **69**: 281-285, 1988.

24. Cox, A. M., S. W. Mendryk, J. F. Kramer and S. M. Hunka. Effect of electrode placement and rest interval between contractions on isometric knee extension torques induced by electrical stimulation at 100 Hz. Physiother. Can. **38**(1): 20-27, 1986.

25. Crow, M. T. and M. J. Kushmerick. Chemical energetics of slow- and fast-twitch muscles of the mouse. J. Gen. Physiol. **79**: 147-166, 1982.

26. Currier, D. P. and R. Mann. Muscular Strength Development by Electrical Stimulation in Healthy Individuals. Phys. Ther. **63**(6): 915-922, 1984.

27. Currier, D. P., C. Reed Petrilli and A. J. Threlkeld. Effect of Graded Electrical Stimulation on Blood Flow in Healthy Muscle. Phys. Ther. **66**(6): 937-943, 1986.

28. Dawson, J. M., D. G. Gadian and D. R. Wilkie. Contraction and recovery of living muscles studied by 31p Nuclear Magnetic Resonance. J. Physiol. **267**: 703-735, 1977.

29. Dawson, M. J., D. G. Gadian and D. R. Wilkie. Muscular fatigue investigated by phosphorus nuclear magnetic resonance. Nature. **274**: 861-866, 1978.

30. Dons, B., K. Bollerup, F. Bonde-Peterson and S. Hancke. The Effect of Weight-Lifting Exercise Related to Muscle Fibre Composition and Muscle Cross-Sectional Area in Humans. Eur. J. Appl. Physiol. **40**: 95-106, 1979.

31. Duchateau, J. and K. Hainaut. Electrical and mechanical failures during sustained and intermittent contractions in humans. J. Appl. Physiol. **58**(3): 942-947, 1985.

32. Edgerton, V. R., J. L. Smith and D. R. Simpson. Muscle fibre type populations of human leg muscles. Histochem. J. **7**: 259-266, 1975.

33. Edman, K. A. and A. R. Mattiazzi. Effects of fatigue and altered pH on isometric force and velocity of shortening at zero load in frog muscle. J Mus. Res. and Cell Mot. **2**: 321-334, 1981.

34. Edwards, R. H. T. New Techniques for studying human muscle function, metabolism, and fatigue. Muscle and Nerve. **7**: 599-609, 1984.

35. Enoka, R. M. Muscle Strength and Its Development: New Perspectives. Sports Med. **6**: 146-168, 1988.

36. Fabiato, A. and F. Fabiato. Effects of pH on the myofilaments and the sarcoplasmic reticulum of skinned cells from cardiac and skeletal muscles. J. Physiol. **276**: 233-255, 1978.

37. Fellenius-Bylund, A., P. Walker, A. Elander, H. S., J. Holm and T. Schersten. Energy metabolism in relation to oxygen partial pressure in human skeletal muscle during exercise. Biochem. J. **200**: 247-255, 1981.

38. Gadian, D. G. "Nuclear magnetic resonance and its applications to living systems." 1982 Clarendon Press. Oxford.

39. Geddes, L. A. A Short History of the Electrical Stimulation of Excitable Tissue. The Physiologist. **27**(1 (Sup): 1984.

40. Gentz, L. and C. Moore. Effect of duty cycle on fatigue during stimulation of the quadriceps muscle. Phys. Ther. **66**(5): 834, 1988.

41. Gollnick, P. D. Peripheral Factors as Limitations To Exercise Capacity. Can. J. Appl. Spt. Sci. **7**(1): 14-21, 1982.

42. Harris, R. C., K. Sahlin and E. Hultman. Phosphagen and lactate contents of M. quadriceps femoris of man after exercise. J. Appl. Physiol. **43**(5): 852-857, 1977.

43. Henneman, E. Recruitment of motor neurons: the size principle. Progress in Neurophysiology. **9**: 9, 1981.

44. Henriksson, J., A. Katz and K. Sahlin. Redox state changes in human skeletal muscle after isometric contractions. J. Physiol. **380**: 441- 451, 1986.

45. Hirvonen, J., S. Rehenen, H. Rusko and M. Harkonen. Breakdown of high energy phosphate compounds and lactate accumulation during short supramaximal exercise. Eur. J. Appl. Physiol. **56**: 253-259, 1987.

46. Hooper, D., R. Miller, R. Layzer, D. Giannini, S. Milner-Brown, A. Koretsky and M. W. Weiner. Correlation between high-energy phosphates and fatigue in human muscle. Society of Magnetic Resonance in Medicine Meeting. **4**: 481-482, 1985.

47. Hultman, E., J. Berstrom, N. McLennan-Anderson and ;. 56. Breakdown and resynthesis of phosphorylcreatine and adenosine triphosphate in connection with muscular work. Scand. J. Clin. Lab. Invest. **19**: 56-62, 1967.

48. Hultman, E. and H. Sjohalm. "Biochemical Causes of fatigue." Human Muscle Power. Jones, McCartney and McComas ed. 1986 Human Kinetics Publishers. Champaign, Illinois.

49. Hultman, E. and H. Sjoholm. Electromyogram, force and relaxation time during and after continuous electrical stimulation of human skeletal muscle. J. Physiol. **339**: 33-40, 1983.

50. Hultman, E. and H. Sjoholm. Energy metabolism and contraction force of human skeletal muscle in situ during electrical stimulation. J. Physiol. **345**: 525-532, 1983.

51. Hultman, E., H. Sjoholm, I. Jaderholm-Ek and J. Krynicki. Evaluation of methods for electrical sitmulation of human skeletal muscle in situ. Pflugers Arch. **398**: 139-141, 1983.

52. Hultman, E. and L. Spriet. Skeletal muscle metabolism, contraction force and glycogen utilization during prolonged electrical stimulation in humans. J. Physiol. **374**: 493-501, 1986.

53. Karlsson, J. Lactate and Phosphagen Concentrations in Working Muscle of Man. Acta Phys. Scand. **Sup 358**: 1-72, 1971.

54. Karlsson, J., C. F. Funderburk, B. Essen and A. R. Lind. Constituents of human muscle in isometric fatigue. J. Appl. Physiol. **38**(2): 208-211, 1975.

55. Katz, A. and K. Sahlin. Regulation of lactic acid production during exercise. J. Appl. Physiol. **65**(2): 509-518, 1988.

56. Katz, A. and K. Sahlin. Role of Oxygen in Regulation of Glycolysis and Lactate Production in Human Skeletal Muscle. Exer. Sci. Sports. Rev. **18**: 1-28, 1990.

57. Katz, A., K. Sahlin and J. Henriksson. Muscle ATP turnover rate during isometric contraction in humans. J. Appl. Physiol. **60**(6): 1839-1842, 1986.

58. Kotz, Y. M. Electrical Stimulation. Canadian Soviet Exchange Symposium on Electrical Stimulation of Skeketal Muscle. Presented at the International Scientific exchange, Concordia University 1977.

59. Kramer, J., D. Lindsay, D. Magee, S. Mendryk and T. Wall. Comparison of Voluntary and Electrical Stimulation Contraction Torques. J. Orthop. Sports Phys. Ther. **5**(6): 324-331, 1984.

60. Kramer, J. F. and S. W. Mendryk. Electrical Stimulation as a Strength Improvemert Technique: A Review. J. Orthop. Sports Phys. Ther. **6**(1): 91-103, 1982.

61. Kramer, J. F. and J. E. Semple. Comparison of Selected Strengthening Techniques for Normal Quadriceps. Physiother. Can. **35**: 500-506,1982.

62. Laughman, R. K., J. W. Youdas, T. R. Garrett and E. Y. S. Chao. Strength Changes in the Normal Quadriceps Femoris Muscle as a Result of Electrical Stimulation. Phys. Ther. **63**(4): 494-499, 1983.

63. Lexell, J., K. Henriksson-Larsen and M. Sjostrom. Distribution of different fibre types in human skeletal muscle. Acta. Physiol. Scand. **117**: 115-122, 1983.

64. Lloyd, T., G. De Domenico, G. R. Strauss and K. Singer. A review of the use of electro-motor stimulation in human muscles. Aust. J. Physio. **32**(1): 18-30, 1986.

65. Magee, D. J. and D. P. Currier. Effects of Number of Repetitions on Isokinetic Kenn Strength. Physiother. Can. **38**(6): 344-348, 1986.

66. Mainwood, G. W. and J. M. Renaud. The effect of acid-base balance on fatigue of skeletal muscle. Can, J. Physiol. Pharmacol. **63**: 403-416, 1985.

67. Massey, B. H., R. C. Nelson, B. C. Sharkey and T. ;. 5. 1. Comden. Effects of High Frequency Electrical Stimulation on the Size and Strength of Skeletal Muscle. Sports Med. and Phys. Fit. **5**: 136-140, 1965.

68. Matheson, G. O. Skeletal Muscle Metabolism: an NMR Study.; P.hD. Thesis, University of British Columbia, 1990.

69. McCully, K. K., B. J. Clark, J. A. Kent, J. Wilson and B. Chance. Biochemical adaptations to training: implications for resisting muscle fatigue. Can. J. Physiol. Pharmacol. **69**: 278-278, 1991.

70. McCully, K. K., J. Kent and B. Chance. Application of 31P Magnetic Resonance Spectroscopy to the Study of Athletic Performance. Sports Med. **5**(3): 312-321, 1988.

71. McMiken, D. F., M. Todd-Smith and C. Thompson. Strengthening of Human Quadriceps Muscles by Cutaneous Electrical Stimulation. Scand. J. Rehab. Med. **15**(1): 25-28, 1983.

72. Meyer, R. A., G. R. Adams, M. F. Fisher, P. F. Dillon, J. M. Krisanda, T. R. Brown and M. J. Kushmerick. Effect of decreased pH on Force and Phosphocreatine in Mammalian Skeletal Muscle. Can. J. Physiol. Pharmacol. **69**: 305-310, 1991.

73. Meyer, R. A. and M. J. Kushmerick. Application of 31P-NMR Spectroscopy to the Study of Striated Muscle Metabolism. Am. J. Physiol. **242**: C1-C11, 1982.

74. Moon, R. B. and J. H. Richards. Determination of Intracellular pH by 31P magnetic Resonance. J. Biol. Chem. **248**(20): 7276-7278, 1973.

75. Moritani, T., M. Muro and A. Kijima. Electromechanical Changes during Electrically Induced and Maximal Voluntary Contractions: Electrophysiologic Responses of Different Muscle Fibre Types during Stimulated Contractions. Exp. Neurol. **88**: 471-483, 1985.

76. Muller, E. A. Influence of training and of inactivity on muscle strength. Arch. Phys. Med. Rehab. **58**(4): 120-129, 1958.

77. Nelson, R. M. and D. P. Currier. "Clinical Electrotherapy." 1987 Appleton and Lange. New York.

78. Packman-Braun, R. Relationship Between Functional Electrical Stimulation Duty Cycle and Fatigue in Wrist Extensor Muscles of Patients with Hemiparesis. Phys. Ther. **68**(1): 51-55, 1988.

79. Paudler, W. W. "Nuclear Magnetic Resonance: General Concepts and Applications." 1987 John Wiley and Sons. New York.

80. Richardson, D. and R. Shewchuk. Effects of contraction force and frequency on postexercise hyperemia in human calf muscles. J. Appl. Physiol. **49**(4): 649-654, 1980.

81. Rose, S. J. and J. M. Rothstien. Muscle Biology and Physical Therapy: A Historical Perspective. Phys. Ther. **62**(12): 1754-1756, 1982.

82. Sahlin, K., L. Edstrom and H. Sjoholm. Fatigue and phosphocreatine depletion during carbon dioxide induced acidosis in rat muscle. Am. J. Physiol. **245**(14): C15-C20, 1983.

83. Sahlin, K., L. Edstrom, H. Sjoholm and E. Hultman. Effects of lactic acid accumulation and ATP decrease on muscle tension and relaxtion. Am. J. Physiol. **240**: c121-126, 1981.

84. Sahlin, K., R. C. Harris and E. Hultman. Creatine Kinase Equilibrium and Lactate Content Compared with Muscle pH in Tissue Samples Obtained after Isometric Exercise. Biochem. J. **152**: 173-189, 1975.

85. Sale, D. and D. MacDougall. Specificity in Strength Training: A Review for the Coach and Athlete. Can. J. App. Sports Sci. **6**: 87-92, 1981.

86. Sale, D. G. "Neural Apaptation in Strength and Power Training." Human Muscle Power. Jones, McCartney and McComas ed. 1986 Human Kinetics. Champaign Illinois.

87. Salmons, S. and J. Henriksson. The adaptive response of skeletal muscle to increased use. Muscle and Nerve. **4**: 94-105, 1981.

88. Saltin, B. and B. Essen. "Muscle Glycogen, Lactate, and CP in intermittent exercise." Muscle Metabolism During Exercise. Pernow and Saltin ed. 1970 Plenum Press. New York.

89. Sapega, A. A., D. P. Sokolow, T. J. Graham and B. ;. 1. (. 4. Chance. Phosphorus Nuclear Magnetic Resonance: a Non-Invasive Technique for the Study of Muscle Bioenergetics during Exercise. Med. Sci. Sports Exer. **19**(4): 410-420, 1987.

90. Sejersted, O. M., J. A.R., K. R. Kardel, P. Blom, O. Jensen and L. Hermansen. Intramuscular fluid pressure during isometric contraction of human skeletal muscle. J. Appl. Physiol. **56**(2): 287-295, 1984.

91. Selkowitz, D. M. High Frequency Electrical Stimulation in Muscle Strengthening. Am. J. Sports Medicine. **17**(1): 103-111, 1989.

92. Selkowitz, D. M. Improvement in Isometric Strength of the Quadriceps Femoris Muscle after Training with Electrical Stimulation. Phys. Ther. **65**(2): 186-196, 1985.

93. Shavelson, R. J. "Stastical Reasoning for the Behavioral Sciences." 1988 Allyn and Bacon. Boston.

94. Shenton, D. W., R. B. Heppenstall, B. Chance, S. G. Glasgow, M. D. Schall and A. A. Sapega. Electrical Stimulation of Human Muscle Studied Using 31P-Nuclear Magnetic Resonance Spectroscopy. J. Orthop. Res. **4**(2): 204-211, 1986.

95. Sjogaard, G., R. P. Adams and B. Saltin. water and ion shifts in skeletal muscle of humans with intense dynamic knee extension. Am. J. Physiol. **248**: R190-196, 1985.

96. Sjoholm, H., K. Sahlin, L. Edstrom and E. Hultman. Quantitative estimation of anaerobic and oxidative energy metabolism and contraction characsitics in intact human skeletal muscle in reponse to electrical stimulation. Clin. Physiol. **3**: 227-239, 1983.

97. Spriet, L., E. Hultman and K. Soderlund. Energy cost of metabolic regulation during intermittent and continous tetanic contractions in human skeletal muscle. Can. J. Physiol. Pharmacol. **66**: 134-139, 1987.

98. Spriet, L., K. Soderlund, M. Bergstrom and E. Hultman. Skeletal muscle glycogenolysis, glycolysis, and pH during electrical stimulation in men. J. Appl. Physiol. **62**(2): 616-621, 1987.

99. Stainsby, W. N. and G. A. Brooks. Control of Lactic Acid Metabolism in Contracting Muscles and during Exercise. Exer..Sci..Sports..Rev.. **18**: 29-63, 1990.

100. Stefanovska, A. and L. Vodovnik. Changes in Muscle Force following Electrical Stimulation. Scand. J. Rehab. Med. **17**: 141-146, 1985.

101 Stuart, D. G. and R. M. Enoka. "Motorneurons, Motor Units, and the Size Principle." The Clinical Neurosciences. Rosenberg ed. 1983 Churchill Livingstone. New York.

102. Taylor, D. J., P. Styles, P. M. Matthews, D. A. Arnold, D. G. Gadian, P. Bore and G. K. Radda. Energetics of Human Muscle: Exercise Induced ATP Depletion. Mag. Res. Med. **3**: 44-54, 1986.

103. Tesch, P. A., B. Colliander and P. Kaiser. Muscle Metabolism During Intense, Heavy Resistance Exercise. Eur. J. Appl. Physiol. **55**: 362-366, 1986.

104. Thompson, L. P. and D. E. Mohrman. Blood flow and oxygen consumption in skeletal muscle during sympathetic stimulation. Am. J. Physiol. **245**(14): H66-H71, 1983.

105. Trimble, M. H. Effects of electrical stimulation on the recruitment order of motor units in man: indirect examination by electrically evoked muscle responses. 1987.

106. Vollestad, N. K. "Motor Unit Recruitment: A Histochemical Approch." Muscular Function in Exercise and Training. Marconnett and Komi ed. 1987 Karger. Paris.

107. Yoshiteru, S., K. Yoshizaki and T. Morimoto. A H-Nuclear Magnetic Resonance Stuky on Lactate and Intracellular pH in Frog Muscle. Jap. J. Physiol. **33**: 721-731, 1983.

Appendix 1.
REVIEW OF LITERATURE

1.1 Electrical Muscle Stimulation

Electrical muscle stimulation produces contraction of skeletal muscle by excitation of peripheral motor nerves using an electrical current source [35]. The current is transmitted through the skin via surface electrodes placed over the muscle (or motor nerve), or delivered directly to the subcutaneous tissue via needle or implanted electrodes. When current of a sufficient intensity reaches a nerve, it depolarizes the nerve's membrane causing propagation of an action potential. Depolarization of a sensory nerve causes the cutaneous discomfort associated with EMS, while motor nerve stimulation produces muscle contraction. Since normal peripheral motor nerves have a lower threshold than the muscle membrane, the membrane is always depolarized via the nerve (when normal innervation is present)[51].

In addition to sensory and motor stimulation, EMS also activates autonomic nerve fibres [104]. During intense voluntary muscle contractions an increase in sympathetic tone produces local vasoconstriction. Normally, local metabolic demand provides a much greater stimulus for vasodilation in the tissues adjacent to the contracting musculature. However, significant increase in sympathetic vasoconstriction in response to high intensity EMS have been observed in canine muscle [104]. The intensity of this autonomic response was

sufficient to significantly reduce blood flow in the contracting muscle tissue [104].

Since EMS produces muscle contraction independent of central neural control muscle response differs from that elicited by voluntary contractions When electrical current of sufficient intensity reaches a motor nerve the resulting depolarization causes complete activation of all muscle fibers within that motor unit. The resulting synchronous activation of all recruited motor units causes the characteristic jerky, involuntary contraction commonly associated with EMS. In addition EMS contractions are localized to the area of current flow, which is often in a relatively small and superficial portion of the muscle. Thus, an EMS induced contraction producing 40% of the muscles maximal voluntary capability (MVC) is probably a result of a select portion of the muscle contracting in a synchronous (maximal) fashion.

During voluntary muscle activation, the force and speed of the contraction is determined by the number of motor units recruited and the firing rate (rate coding) of the recruited fibers [106]. The selection of motor units is mediated by the strength of supraspinal or peripheral stimuli required to discharge a given motoneuron.[101] This functional threshold increases in proportion to the size of the motoneuron [43].

Muscle units, the muscle fibers innervated by a specific motoneuron, can be classified by their histochemical and morphological properties [101]. Homogeneous types of muscle fibers are present with a motor unit, and may be classified as; slow oxidative (S.O.), fast fatigue resistant (F.R.), fast intermediate (F.Int.) and fast fatiguable (F.F.). In mammals the size of the motoneuron increases as the glycolytic capacity of the

fiber increases [43]. Thus, during voluntary contractions, small motoneurons which primarily innervate slow oxidative fibers are recruited first, followed by larger (more glycolytic) motor units [101]. This orderly recruitment pattern has been observed through a wide range of intensities during isometric and dynamic contractions in humans [106].

It is often stated that direct application of electrical current to motor nerves (as with EMS) preferentially depolarizes the large diameter motor fibers associated with fast glycolytic fibers. Despite the fact that this phenomenon has never been directly (experimentally) demonstrated considerable empirical and indirect evidence of reversed recruitment does exist [35].

In contrast to voluntary contractions the threshold of peripheral motor axons to external current varies inversely with the size of the axon [101]. This response is a result of myelin sheath architecture and causes large axons to be depolarized before small axons [101]. In addition, these large diameter motoneurons are often located in a superficial portion of the muscle, closer to the current field produced by transcutaneous EMS [63].

The associated afferent cutaneous simulations produced by EMS may also play a role in altering recruitment order [105]. Cutaneous simulation has been shown to increase time to peak tension of the twitch response during the human Hoffman reflex [105]. This may indicate that a faster group of motor units had been recruited for the reflex response in the presence of EMS.

The probable alteration of recruitment order by EMS has significant implications for may areas prospective EMS use, such as the functional EMS programs currently being developed for assisted ambulation in spinal cord patients. However, the significance of this response for most uses of EMS in clinical rehabilitation is dubious. EMS used to strengthen skeletal muscle is typically applied for a short duration at the maximal current intensity tolerated by the patient [91]. The intensity of the applied current is usually in the order of 20-50 milliamps [16]. Since reported depolarization thresholds for fast and slow twitch motoneurons are between 5 and 20 nanoamps (10^{-3} amps)[101] it seems likely that all motoneurons in the area of current flow will be recruited.

EMS training studies have reported preferential adaptation of fast glycolytic fibers post training [17]. However the authors concluded that these adaptations could have been a result of the "strength" (high intensity/short duration) nature of the EMS contractions, and not necessarily a result of preferential fiber recruitment by the electrical current [17]. Similar adaptations have been reported following voluntary training programs utilizing short duration high intensity contractions [23].

Activation of motoneurons at a constant frequency during EMS differs from the variable activation frequency exhibited during voluntary contractions [10]. During sustained voluntary contractions the discharge frequency of motor nerves declines in an effort to maintain force production and prevent electrical propagation failure [10]. However the motor neuron discharge rate during EMS induced contractions is determined by the stimulator frequency, and remains constant

throughout the stimulation session. This inability to adapt to changing metabolic conditions within the muscle may accelerate the fatigue response of muscle to EMS contractions.

1.1.1 Current Parameters

Alterations in the type of current applied to the tissues can dramatically effect the sensory and motor response elicited by the electrical current. Current parameters which can alter muscle contraction include: current phase, pulse width, pulse shape, pulse charge, current frequency, pulse interval and current intensity [77].

Pulse width is the amount of time the current flows in one direction from the zero baseline (figure 22a), while pulse charge is the quantity of current delivered to the tissue . The pulse charge is represented by the area under each pulse shape (figure 22b). If areas under each half of the pulse differ, a net positive or negative charge results. The vast majority of manufactured muscle stimulators produce an alternating current referred to as biphasic, since the current travels in in a positive and negative direction from the zero baseline (figure 22). When an equal amount of current flows on each side of the zero baseline, the resulting 'net zero' wave does not produce specific ion buildup in the tissues beneath the electrodes [6].

The pulse interval is the length of time between pulses (figure 22c). Frequency refers to the number of stimuli delivered in one second, measured in hertz. Peak intensity is represented by the height of each pulse and is measured in milliamps. These variables are often manipulated in an effort to maximize the motor response while minimizing the associated sensory irritation.

The width of each pulse affects the subjective comfort of the stimulation [64]. As the width of the pulse increases, so does the sensory nerve stimulation, and thus discomfort beneath the electrodes. Alon et al [3] determined that the optimal pulse width for motor stimulation of human biceps brachii was between 0.02 - 0.2 milliseconds. Hultman et al [51] found that increasing the pulse with from 0.2 to 1 milliseconds produced a linear increase in force production in the human quadriceps. In contrast, pulse widths greater than 1 millisecond failed to produce greater muscular force production [51].

Pulse shape refers to the geometric pattern of each pulse (eg. square or triangular wave) based on the relationship of the shape of each half of the pulse. Pulse shape does not seem to have a major effect on the muscle response in terms of tension generated [64]. However, it is thought that a fast rising pulse (i.e. square wave) may produce a stronger contraction than a slower rising pulse (i.e. triangular wave)[64].

The minimal frequency (pulses per second) required to produce a tetanic muscle contraction is between 20 and 50 hertz [6] Mammalian muscle exhibits a wide range of firing frequencies among motor units. Tetanic contraction of slow units may be elicited at frequencies a low a 8 Hz, while fast units may require 80-100 Hz [9]. In fast contracting human muscles (biceps brachii, adductor pollicus) firing rates may range from 12-50 Hz, with an average of 30 Hz [9].

Clinically, EMS frequencies between 30 and 80 Hz are commonly utilized [77]. However, stimulation frequencies above 50 Hz may result in rapid reduction in muscle force output associated with electrical transmission failure [9]. Moritani et al. showed that electrical

stimulation of the human gastrocnemius at 50 and 80 Hz resulted in a significantly greater force decline than a maximal voluntary contraction of 60 seconds duration. The rapid decline in the amplitude and width of surface EMG potentials recorded during EMS contractions lead the authors to hypothesize that electrical propagation failure was responsible for the difference in fatigue response between voluntary and EMS induced contractions [75].

Traditionally the intensity of an EMS induced contraction (figure 22d) has been expressed as a percentage of the muscles maximal voluntary isometric force capability (MVC) generated by a given intensity of stimulation. Pain resulting from cutaneous nerve stimulation is the most common limiting the tolerance of EMS intensity [59] Clinicians alter current parameters, electrode position and skin preparation in order to elicit the highest possible current tolerance and force output from the stimulated muscle. Intensities of EMS contractions in recent training studies range from 5%[100] to over 100%[59] of MVC. Results of numerous EMS training studies show that the increase in isometric strength is positively correlated with the intensity of current applied, as measured by percent of MVC (for review see Selkowitz [91]).

However, as mentioned previously, during an EMS induced contraction synchronously activated fibers are localized to the area of current flow. Thus, a 30% MVC contraction represents a 100% activation of a relatively small portion of the muscle. Hultman and Spriet calculated that a 20 Hz current producing a 26% MVC contraction of the human quadriceps resulted in activation of 35-37% of the knee extensor muscle fibers [52].

Figure 22
Current Waveform

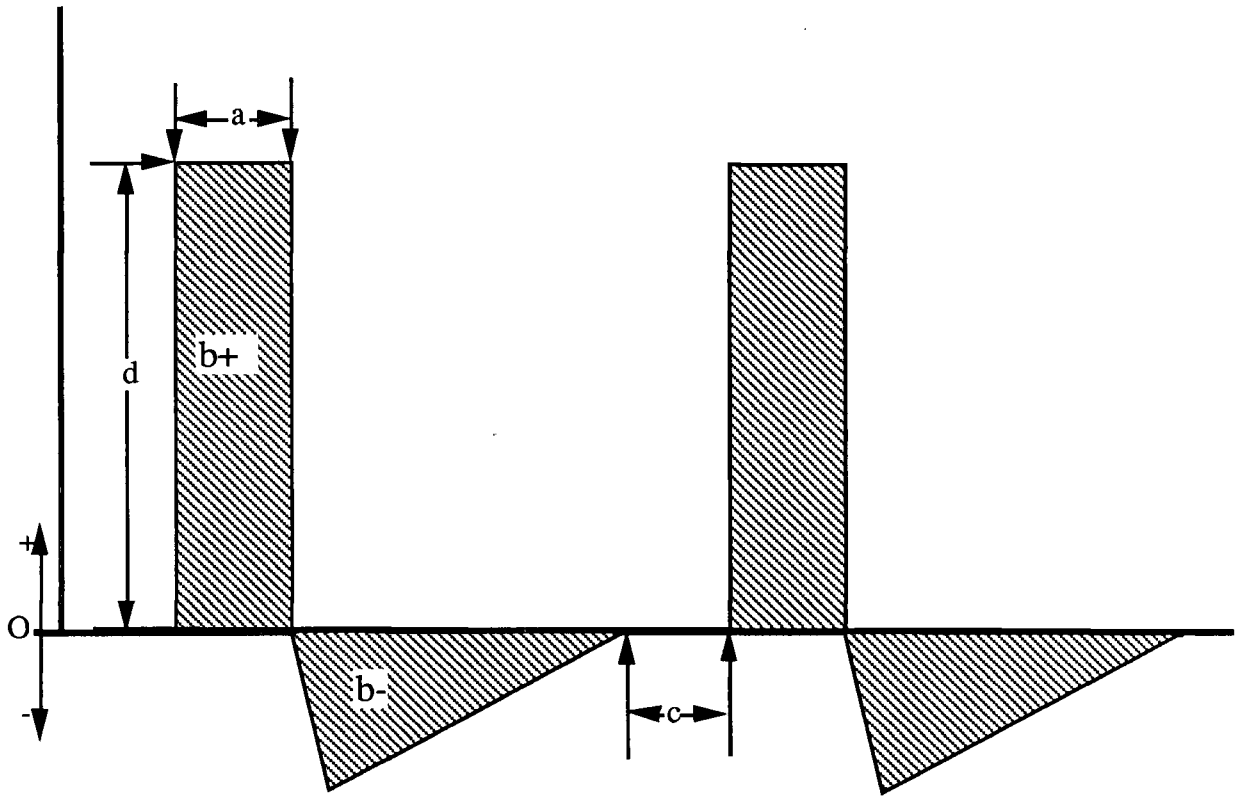

Asymetrical Biphasic square wave, where: a) Pulse width represents the amount of time the current flows in one direction from the zero baseline. b) Pulse charge is illustrated by the areas (+ and -) under each pulse shape. Equal positive and negitive areas prevents ion buildup in the tissues. c) Interpulse interval and d) Current intensity.

1.1.2 Application Protocols

The application of a given EMS current can be defined in terms of: length of contraction, length of rest period, and number of contractions. The ideal stimulation protocol will produce repeated high intensity contractions (overload) and therefore, a training effect, for a specific number of contractions.

Muscle weakness has been described as a failure to generate the required force output, whereas, fatigue is the failure to maintain required force output [34]. Thus, a progressive decline in force output over a series of intermittent contractions represents muscle weakness, while, failure to maintain force output during a given contraction represents fatigue. In investigations of diseased and normal muscle events within the; electromechanical activation system, the contractile machinery and metabolic fuel supply have all been implicated in the production of weakness [34]. In contrast, a reduction in central and peripheral neural activation, or impaired excitation/contraction coupling have been associated with the development of fatigue [34].

Inducing weakness early within the set of contractions serves to reduce the quantity of training stimulus. Bigland-Richie, Jones and Woods [10] studied the relationship between EMS frequency, contraction duration, and Electromyographic (EMG) activity in the human adductor pollicus muscle. Above 50 hertz, the motor unit activity began to decline rapidly after 10 seconds of stimulation. Moritani [75] observed a similar response in the human gastrocnemius, with tension decline occurring in less than 10 seconds at 80 Hz. Both investigators implicated electrical propagation failure as the mechanism for this "high frequency" fatigue [9, 75].

Although it appears that no specific evaluation of length of EMS induced contraction on training response has been conducted, it seems that contractions of less than 10 seconds would provide an adequate training response while avoiding fatigue associated with conduction failure, regardless of the stimulation frequency utilized. In a study of

isometric voluntary contractions, Muller [76] found that increasing the duration of the isometric contractions from one to six seconds increased and accelerated strength gains.

Prior to the late 1970's there was no single commonly used protocol in EMS strength programs. In 1977, Yakov Kotz described what has come to be known as the 10/50/10 protocol [58]. The protocol was developed following investigation of the effect of 40 and 50 second rest periods between EMS induced contractions of normal biceps brachii and calf muscles in humans. Kotz advocated the use of 10x10 second maximal electrically induced contractions, each followed by a 50 second rest period. He stated that 10 seconds represented the greatest length of time a maximal EMS contraction could be sustained, while 50 seconds represented the minimal rest time before another maximal EMS contraction could be induced. Despite the dearth of reproducible experimental data, this protocol subsequently became widely used in clinical rehabilitation.

Using what is thought to be a similar current format to that of Kotz, Currier and Mann [26] reported a 20% torque decrement following 10 ten second maximal EMS induced contractions. In contrast subjects quadriceps torque output declined only 10% following the same number of voluntary contractions. The magnitude of fatigue generated by EMS ,compared to voluntary, contractions may indicate that greater mechanical or metabolic stress is applied to the active fibers during EMS. Cox et al [24] compared the reduction in torque production associated with 35, 50 and 60 second rest periods between 10 second maximal EMS induced contractions of the Quadriceps muscle. No statistically significant difference was observed between the 50 and 65 second

intervals. However the 35 second interval did produce greater torque reduction than the 65 second rest interval. In a study of EMS training of the quadriceps Selkowitz [92] found it necessary to provide a 120 second rest interval if force output during maximal 10 second EMS induced contractions was to be maintained.

In their clinical guide to electrical stimulation Baker et al published results of an investigation of the force output of the human peronei stimulated via implanted electrodes [6]. The results showed that a one second on one second off protocol produced rapid decline in muscle force in three minutes, while a one second on/five seconds off pattern provoked no force decline in 30 minutes. Shenton et al investigation of changes in intramuscular energy metabolism associated with tetanic and subtetanic electrical stimulation showed that a work/rest ratio of less than 1:2 was sufficient to maintain muscle force output over ten contractions [94].

Recently Packman-Braun evaluated the response of forearm extensors in hemiplegic patients to alterations in the rest period between ten second EMS induced contractions [78]. The 10 sec on/10 sec off protocol reduced force output by 50% within 10 minutes, while the majority of the 10/50 protocol group maintained >50% of initial force for over 30 minutes [78]. Unfortunately these results must be viewed as specific to the sample population since hemiparesis produces a specific atrophic pattern in the effected musculature, which may alter the muscles fatigue response. [21].

It is clear that alterations in the length of inter-contraction rest period has a significant effect on the mechanical response of muscle during

repeated contractions. In addition, extensive investigations of the metabolic response to intermittent electrically induced and voluntary maximal contractions have been conducted. Increase in muscle lactate accumulation and decline of force production are associated with increasing the duration of individual stimulation bouts with a constant work/rest ratio [88]. Results of investigations by Duchateau [31], Saltin [88], and Baker [6] indicate that a work/rest ratio of 1:1 or less results in rapid force decline associated with intramuscular acidosis. However, results reported by Shenton et al indicates that a work/rest ratio of 1:2 was sufficient to facilitate constant force production over the course of 10 contractions [94].

There appears to be no scientifically based rationale for the selection of the number of EMS contractions used in a given training session. However, an evaluation of the effects of the number of repetitions of isokinetic knee extension and flexion on muscle strength was conducted by Magee and Currier. No significant difference in strength gain was observed between six groups that performed between 6 and 12 repetitions [65].

1.1.3 Clinical Efficacy of Electrical Muscle Stimulation

While some studies have shown that isometric EMS training is as effective as voluntary isometric exercise in increasing isometric strength, other investigators have failed to confirm this. The wide variation in the stimulation protocols and parameters utilized in these studies makes integration of these conflicting results difficult. Kramer and Semple [61] compared the effectiveness of voluntary, electrically stimulated and superimposed contractions in increasing isometric strength over four

weeks of training. The authors reported gains of 19%, 13% and 12% for the voluntary, EMS and superimposed groups. Laughman's [62] comparison of voluntary and EMS training over a five week period yielded a 22% isometric strength gain in the EMS group compared to 18% in the voluntary group. A similar comparison by McMiken [71] yielded a 22% and 25% isometric strength gain in the EMS and voluntary groups respectively. In contrast, Massey [67] reported that EMS was not as effective as voluntary isometric exercises or isotonic weight training in improving isometric or isotonic strength after nine weeks.

1.2 Energy Metabolism during Exercise

Skeletal muscle comprises 40% of human body mass [34]. This sizable tissue mass is able to meet a wide array of functional demands by virtue of its extensive metabolic range. Maximally activated muscle can increase its energy expenditure by over 400%[57]. In addition, skeletal muscle exhibits considerable plasticity, adapting, (structurally and metabolically) to a wide range of functional demands [81].

Adaptation to the performance of high intensity contractions for short time periods occurs primarily within the muscles' contractile protein structure [7]. These structural modifications are induced by repeated high intensity/short duration contractions [5]. Contractions designed to enhance muscular force production must produce more than 50% of the muscles maximal output to be efficacious [30].

Training programs designed to accelerate this type of muscle adaptation can elicit repeated high intensity contractions by incorporating inter-contraction rest periods. Since complex metabolic processes are responsible for converting chemical energy to high

intensity mechanical work, some understanding of the energy transduction process in this type of muscular exercise is obligatory.

Contraction of skeletal muscle is initiated by activation of the peripheral motor nerve [34]. Following nerve activation the muscle membrane is depolarized via stimulation across the neuromuscular junction. In turn, membrane depolarization results in calcium release from the sarcoplasmic reticulum into the cytoplasm.[14]. The formation of a calcium-troponen complex facilitates the coupling of actin and myosin [14]. The energy required to promote actin/myosin coupling (and uncoupling) is derived from adenosine triphosphate (ATP) hydrolysis [8].

$$\mathbf{ATP \dashrightarrow ADP + P_i + Contraction}$$

In addition, ATP is hydrolyzed to run the calcium and sodium pumping systems which maintain the intracellular environment [8]. Since ATP is only present in limited quantities within the cell (4.5 mmol/kg/dm [41]), constant replenishment of this high energy metabolite is necessary [57].

The ATP required to produce and sustain muscle contraction is derived from three sources [53]. The principle energy source utilized for a given activity is dependant on the intensity, duration and type of muscle contraction employed [14].

Creatinephosphate (PCr) in the cytoplasm serves as an immediate/short term ATP source via the creatine kinase (CK) reaction [20];

$$\mathbf{ADP + PCr \xrightarrow{CK} ATP + Cr}$$

Speed of creatine phosphate breakdown is dependant on the intensity of muscle work [45]. During maximal muscular exercise the small (15 mmol/kg/dm [41])intramuscular PCr stores are exhausted within five to seven seconds [45]. ADP re-phosphorylation via glycolysis begins within a few seconds of muscle activation [44, 53]. Glycolysis involves the breakdown of six carbon sugars in the cytoplasm, such that [89];

$$\mathbf{Glycogen_n + 3\ ADP + 3P_i \dashrightarrow PME\ Glycolytic\ Intermediates \dashrightarrow Glycogen_{n-1} + 3\ ATP + 2\ Lactate}$$

The above reaction depicts what is often termed anaerobic glycolysis, which produces lactate. Technically speaking the endpoint of glycolysis may be pyruvate or lactate, depending on the metabolic conditions within the cell [56]. Considerable controversy currently exists regrading the activation and control of glycolysis [12, 13, 55, 56, 99]. Initial activation of the glycolytic pathway probably occurs with calcium stimulation of glycogenolysis at the onset of contraction [99]. However, activation of glycolysis may also be a response to rising intracellular levels of inorganic phosphate resulting from PCr breakdown [53] The subsequent conversion of pyruvate to lactate occurs via a reaction catalyzed by lactate dehydrogenase (LDH)[14];

$$\mathbf{Pyruvate + NADH + H^+ \xleftrightarrow{LDH} Lactate + NAD^+}$$

The concentration of NADH in the cytosol, which is in turn dependant on the redox state of the mitochondria, is the primary metabolic determinant of the activation of the LDH reaction [99]. The formation of lactate in muscle is dependant, to some extent, on exercise intensity. During whole body exercise at 40% $VO_{2\ max}$ the rate of glycolysis may

increase 25 times [56], however, lack of lactate accumulation in the muscle or blood suggests the successful aerobic metabolism of pyruvate. In contrast, workloads exceeding 50-60% $VO_{2\ max}$ result in a rapid and significant accumulation of lactate in working musculature [53].

Traditionally, the availability of oxygen within the cell was thought to be the primary determinant of the fate of pyruvate [57]. In the presence of adequate oxygen, pyruvate and NADH are shuttled into the mitochondria where they are aerobically metabolized via oxidative phosphorylation [89];

$$\mathbf{NADH + H^+ + 1/2\ O_2 + 3\ ADP + 3\ P_i \text{ ---> } 3\ ATP + NAD^+ + H_20}$$

Although alternative mechanisms for the control of glycolytic metabolism during submaximal exercise have been proposed [12, 99], lack of intramuscular oxygen is acknowledged to limit oxidative phosphorylation during maximal and high intensity isometric contractions [12, 56, 99].

Based on mitochondrial function, five metabolic states have been assigned to working muscle by Chance [20]. At rest (state 4) slow aerobic metabolism predominates, with high substrate levels and low ADP levels. During submaximal muscle contractions aerobic metabolism meets the muscles energy requirements (state 1-3) However, when the oxygen supply to working muscle is limited anaerobic metabolism predominates and the muscle is said to be in state 5 [20].

The mechanical characteristics of isometric muscle contractions give rise to unique metabolic circumstances. Occlusion of local blood flow occurs during voluntary isometric contractions producing external force

greater than 30% of maximal voluntary capacity (MVC)[80]. In fact occlusion of microvascular supply by mechanical pressure from adjacent myofibrils may occur at pressures as low as 30 Torr(15% MVC)[90]. Under these conditions ATP is primarily derived from PCr hydrolysis and glycolysis since only a small amount of oxygen is available from myoglobin, capillary blood O_2 and dissolved O_2 (2mmol/kg/dm [44])[66]. Studies of human quadriceps show that intracellular oxygen supplies are exhausted within five seconds [44]. Lactate production in anoxic isometrically contracting muscle is the primary energy source, accounting for 60% of the ATP turnover [57]. Considering that glucose storage within skeletal muscle is minimal, glycogen is likely the primary substrate for glycolysis under these conditions [41]. Analysis of metabolic response of human quadriceps to EMS induced isometric contractions revealed that glycogenolysis always exceeded glycolysis [50].

Investigations of electrically induced intermittent isometric contractions of the human plantar flexors (30% MVC) indicate that normal increases in regional blood flow associated with exercise does occur, however, capillary flow during contractions is probably still arrested [27].

Since the mechanical muscle response to EMS differs from those observed during voluntary contractions, the metabolic response should also be viewed as unique. In practice, the synchronous, constant frequency, nature of electrically induced contractions is more amenable to the production of isometric (as opposed to isotonic) contractions. Thus the vast majority of EMS use in the laboratory and the clinic, consists of isometric contraction production.

2.2.1 Metabolic Response to Electrical Muscle Stimulation

Hultman's study of isolated electrically stimulated muscle showed that the ATP utilized during the first 1.5 seconds of a maximal tetanic contraction was derived 80% from PCr and 20% from lactate [47] The subsequent second of contraction resulted in an equal contribution between PCr breakdown and anaerobic glycolysis. During the first six seconds of a maximal contraction, greater than 50% of the ATP used was derived from lactate production. As intramuscular lactate accumulated, the muscle power output began to decrease despite having 65% of its original PCr level remaining.

A subsequent evaluation of the response of the intact human quadriceps muscle (circulation occluded) to EMS applied in a 1.6 seconds on/1.6 seconds off pattern was conducted by this group [50]. Biopsy analysis showed that PCr was almost totally depleted after 40 seconds of contraction, while lactate values continued to rise during the entire 83 seconds of stimulation. Muscular force production declined to 19% of initial output following 83 seconds of stimulation, with the greatest drop occurring after complete PCr depletion at the 40 second mark [50]. Interestingly, the calculated ATP turnover rate declined slowly for the first 40 seconds of stimulation with PCr and glycolysis contributing equally to ADP rephosphorylation during the first 20 seconds. Following PCr depletion after 40 seconds of stimulation the ATP turnover rate began to decline rapidly to below 50% of initial values after 83 seconds of stimulation.

Investigations of glycolytic metabolism commonly collect metabolic data from muscle with occluded circulation, since analysis of a closed

system nullifies the contribution of oxidative metabolism to energy production. However, this type of model bears little relationship to clinical rehabilitation, thus, analysis of the metabolic response of human muscle with open circulation conducted by Hultman [50] is of considerable interest. Application of identical stimulation parameters (to the study discussed above) produced similar force decline, and substrate utilization, to those observed during the first 40 seconds of stimulation of muscle with occluded circulation. However, between 40 and 83 seconds of stimulation, significantly less force decline and lactate accumulation occurred in the muscle with open circulation. Interestingly, a small increase in PCr and ATP was observed in the second half of this open circulation protocol. The authors suggested that aerobic metabolism of carbohydrates produced the increase in energy rich phosphogens in the second half of this open circulation protocol [50].

Shenton et al [94] used NMR spectroscopy to study human forearm flexor metabolism during voluntary and EMS contractions with open circulation. Results showed that EMS contractions caused a extremely rapid depletion of PCr during the first second of a contraction, and a slower drop for the remainder of a six second contraction. During maximal voluntary isometric contractions the PCr drop was three times slower than during the EMS contraction. Recovery of PCr stores was exponentially related to the amount of depletion, with 10% recovery in 8 seconds and full replenishment in 120 seconds. Ten repetitions (6 second on/10 second off) of EMS resulted in a 60% reduction in intramuscular PCr while maximal voluntary isometric and isokinetic resulted in a 66% and 68% reduction respectively.

1.2.2 Intermittent Contractions

Significant differences exist between the metabolic response of muscle to continuous and intermittent EMS protocols. Generally, the repeated activation and relaxation associated with intermittent contractions results in a greater energy cost (per unit contraction time) compared to a continuous contraction [8, 97]. Bergstrom reported the the energy cost of muscle activation and relaxation accounted for 37% of the total energy cost of a 1 second tetanus [8]. Biopsy analysis of human quadriceps revealed that the energy cost of 51 seconds of intermittent EMS induced contractions (1:1 work/rest ratio) was 39% greater than that of continuous stimulations for the same duration [97]. Spriet [97] speculated that the energy cost of calcium transport during relaxation accounted for the majority of the increased energy cost associated with intermittent contractions.

Intermittent contraction protocol consist of two components; contraction (work) and rest. The relationship between these two variables (work/rest ratio) significantly effects the metabolic response of muscle to stimulation [20].

Analysis of intermittent supramaximal (voluntary/isotonic) exercise at a 1:2 work/rest ratio revealed insignificant lactate accumulation following performance of repeated 10 or 20 second work bouts for 30 minutes [88]. However, repeated 30 and 60 second workbouts with the same work/rest ratio produced significant muscle lactate accumulation after 10 minutes. This data suggests that, despite a constant work/rest

ratio, the duration of the workbout has a significant effect on the metabolic response of the active musculature.

Alterations in inter-contraction rest period does not effect the energetics of each contraction, but rather alters the magnitude of recovery, and thus, the energetic state of the active muscle cells prior to each subsequent contraction. During submaximal isokinetic forearm exercise application of a 1 second on/5 seconds off protocol facilitated aerobic metabolism without significant glycolytic activity [20]. Chance suggested that during the inter-contraction rest period, the mitochondria were able to restore normal levels of PCr/Pi, without significant contribution from anaerobic glycolysis [20]. The duration of the rest interval during which the mitochondria function at full capacity increases as the intensity of each contraction increases. Human calf exercise at maximal and supramaximal intensities, produced maximal mitochondrial function over the entire 5 second rest period, accompanied by progressive PCr depletion and maximal glycolysis [20] The synchronous, fixed frequency activation of muscle by tetanic electrical stimulation would surely produce this non-steady state response

1.2.3 Energy Metabolism and Fatigue in Skeletal Muscle

The mechanisms which result in the inability of muscle to attain, or maintain, a given contractile force have long been the subject of intense interest [20, 34, 48, 54]. As discussed previously, activity induced changes in electrical activation, excitation/contraction coupling, and energy metabolism have all been implicated in the production of fatigue and weakness [34]. Research into the metabolic component of fatigue

associated with maximal isometric contractions, have uncovered a complex and multifactorial process [48]. To date, there is no universal agreement on the exact mechanisms of fatigue [29].

A decline in muscular force output can be mediated by two elements of the metabolic process; substrate depletion, and product accumulation [99]. Investigations of the energetics of maximal isometric contractions revealed that significant fatigue develops in the working musculature despite the presence of adequate glycogen concentrations [1]. Some investigations into the role of high energy phosphates in muscular fatigue production have described a close association between intramuscular [PCr] and force production [52]. In a series of experiments conducted by Sahlin et al [83] isolated frog muscle was poisoned with indoacetic acid in order to block glycolysis and prevent lactate formation. Maximal electrical stimulation of this muscle resulted in rapid force decline associated with a sharp drop in [PCr]. When PCr stores were exhausted irreversible rigor developed, illustrating the potential for insufficient ATP supply (via PCr) to produce fatigue. However, fatigue developed in unpoisoned muscle far in advance of ATP depletion [83]. A number of subsequent studies have shown that the relationship between [PCr] and fatigue is far from clear [8, 28, 46].

Although PCr depletion produces isometric force decline [50], low [PCr] has been observed at a wide range of force levels following isometric work [8]. In fact, decline in force output, and an increase in [PCr] have been observed simultaneously in maximally contracting muscle with open circulation [50]. Thus, it appears that substrate depletion does not play a central role in fatigue development during brief maximal isometric contractions.

Changes in intracellular pH (pH_i) secondary to lactate accumulation have long been viewed as a culpable cause of fatigue [53, 54, 66]. Recently many studies of voluntary and EMS induced isometric contractions have associated changes in pH_i with a reduction in muscular force production [33, 53, 54, 66]. However, many investigators are quick to point out that despite the consistent association between cellular acidosis and decreased muscular force output, acidosis may not be the cause of fatigue per se [56, 66]

During muscle contraction acids are produced by both oxidation (CO_2) and glycolysis (HLA)[66]. The subsequent pH change is dependant on the proton load on the cell and the intracellular buffering capacity. The amount of proton production can be expressed as moles of H^+ produced per moles of ATP generated, with glycolysis generating a much greater proton load (0.66x rate of ATP production) than oxidation (0.14x)[66]. In contrast PCr acts as a proton sink, taking up 0.5 mol of H^+ per mol of PCr [66]. The intracellular buffering capacity in mammalian muscle generates a linear relationship between proton load and intracellular pH (at pH values between 6.0 and 7.0)[66]. Thus, the net rate of H^+ production is dependant on the rate of ATP synthesis via glycolysis and PCr breakdown, and the rate of ATP utilization [66].

Within a physiological pH range lactic acid almost completely dissociates into hydrogen and lactate ions [12]. Investigations utilizing proton NMR of isolated muscle have demonstrated that $[H^+]$ is directly proportional to lactate accumulation within the cell [107]. Biopsy of the human quadriceps (circulation occluded) following isometric contractions also reveal a linear relationship between lactate and $[H^+]$ [84]. In vivo,

the accumulation of lactate within the active cells is dependant on lactate removal mechanisms, while the relationship between, pH and proton load is dependant on the intracellular and extracellular buffering capacity [66]. However, the closed extracellular system created by a maximal isometric contraction inhibits lactate efflux , and neutralizes the effects of extracellular buffers. In this situation, H^+ uptake by the creatine kinase reaction would account for 90% of the metabolic buffering potential [98].

The precise association between intracellular acidosis and fatigue is difficult to describe since so many alterations in cellular physiological processes are occurring at the onset of fatigue. As a result of this close interplay investigators have difficulty isolating one dependant variable. However, numerous investigations into this association have revealed several mechanisms by which acidosis produces fatigue [50, 66, 99].

Phosphofructokinase (PFK) is recognized as a key rate limiting enzyme of glycolysis [14]. PFK activity is diminished by a reduction in intracellular pH, which in turn reduces the cellular glycolytic rate [82, 99]. If conditions did not permit oxidative ATP production, this could result in a reduction contractile force secondary to ATP depletion. However, fatigue associated with intracellular acidosis has been observed in the absence of ATP depletion (following short maximal isometric contractions, thus, other mechanisms must contribute to the production of fatigue in these circumstances [50, 98].

Following an investigation of continuous and intermittent EMS induced quadriceps contractions, Hultman [50] concluded that intracellular acidosis may produce fatigue by acting directly at the contractile

machinery, inhibiting calcium transport or calcium binding to troponen. Inhibition of calcium transport and/or binding as a cause of fatigue (in skinned fiber preparations) was also described by Fabiato and Fabiato [36]. In addition a reduction in velocity of shortening of EMS induced frog muscle contractions has been associated diminished pHi [33]. It was hypothesized that a reduction in the affinity of calcium for troponen was responsible for the decrease in the rate of crossbridge cycling [33].

Besides these two direct effects of cellular acidosis on muscular force production some heretofore undefined indirect effects have also been postulated. Experiments using $C0_2$ to increase intracellular proton load have reported an reduction in muscular force output in association with a decrease in intracellular pH [82]. However, the 30% reduction in force was significantly less than the force decline observed during similar proton loads at physiological fatigue (70%). This presents the possibility that reduced pH_i at physiological fatigue is only directly responsible for 40% of the observed reduction in force, while the interaction between acidosis and associated biochemical processes account for the remainder of observed fatigue.

1.2.4 Metabolic Recovery

During maximal intermittent isometric exercise biochemical events during the inter-contraction rest periods have a profound effect on the muscles response during the subsequent contraction [20]. In addition the sequence of metabolic events which returns the muscle cell to a normal resting state following maximal exercise may provide some insight into the biochemical mechanisms of fatigue.

Following maximal isometric work muscle cells are depleted of PCr and exhibit high [H^+] values [94]. During recovery, the rate of oxidative phosphorylation within the mitochondria remains accelerated for a short period, partially to supply the ATP necessary to resynthesize PCr [4]. Resynthesis of PCr via the creatine kinase reaction produces hydrogen ions, which maintains a high intracellular proton load during the early phase of recovery [4, 66, 102]. The resulting drop in pH following exercise has been associated with a drop in contractile tension [66]. Normalization of pH_i and substrate levels is closely correlated with recovery of contractile force following maximal EMS induced contractions [49]. Since [PCr] is restored by oxidative processes, adequate blood supply is essential [94, 96, 102].

The half time of full PCr recovery varies inversely with the intensity of the exercise performed [4, 42] The concentration of PCr during any instant of recovery is primarily dependant on pHi [4]. Arnold [4] observed an exponential recovery of 50% of resting [PCr] in 2 minutes following moderate isotonic forearm exercise. In contrast Taylor reported that PCr resynthesis following exhaustive forearm exercise exhibited a biphasic pattern [102]. [PCr] returned to 70% of resting levels within 3 minutes of cessation of exercise, with full recovery not occurring for over 12 minutes [102]. Sjoholm reported a similar pattern of PCr recovery following EMS application to the human quadriceps [96]. The initial stage of recovery produced 50% PCr resynthesis within 20 seconds and was associated with a rapid increase in twitch relaxation time [96]. The author speculated that increased relaxation time was a result of reduced ATP availability, which was alleviated by PCr

resynthesis [96]. These results illustrate the close relationship between biochemical and mechanical events during recovery.

The recovery of pH_i is dependant on intracellular active transport mechanisms [4] and local blood flow [37]. Prolonged recovery periods following repeated intense contractions have been reported in tissue with impaired blood supply secondary to peripheral vascular disease [37] or tourniquet application [94]

1.3 Nuclear Magnetic Resonance

The major difficulty in establishing physiological guidelines for the use of certain electrical stimulation protocols is related to the relatively gross measurements of strength gain commonly used to assess efficacy. Whole body experiments in humans designed to study oxidative phosphorylation and anaerobic glycolysis during muscle stimulation rely on: (i) indirect whole blood measures of the relevant substrates and metabolites involved, (ii) tissue sampling by muscle biopsy, or (iii) performance measures such as isokinetic dynamometry. Blood metabolites in arterial and venous blood do not always reflect the state of affairs in the sarcoplasm and mitochondria since they represent crude estimates of intracellular bioenergetic events [19]. Muscle biopsies provide metabolic quantification using conventional methods but are painful, destructive and slow, making repeated measures designs impractical. In addition, if sample freezing is not instantaneous, shifts will occur in the concentration of cellular metabolites [19]. These limitations may be eliminated by continuous real time monitoring of intramuscular energy metabolism using nuclear magnetic resonance spectroscopy - NMRS.

1.3.1 Magnetic Nuclei

Atomic nuclei containing odd numbers of protons or neutrons possess a magnetic moment. These odd numbered intranuclear particles produce a net angular momentum within the nucleus, causing the nucleus to behave like a miniature dipole magnet[79]. NMR spectroscopy provokes interaction between nonionizing electromagnetic radiation (in the radio frequency range of 1-500 Megahertz) and these magnetic nuclei[38]. Radiation absorbed, and subsequently emitted, by these nuclei during exposure to a uniform, static magnetic field contains information regarding the quantity of these nuclei within the sample under investigation [89].

The magnetic properties of atomic nuclei are dictated by their spin quantum number (I), and magnetic moment (μ)[79]. The spin quantum number will be a half integral value if the mass number of the nucleus is odd(eg; ^{31}P;I=1/2)[79]. The magnetic moment of a nucleus is dependant on the charge and mass of the nuclear protons [79]. A nucleus with a spin quantum number of zero possesses no magnetic moment. Interestingly, only about one third of all the different isotopes have nonzero spin quantum numbers [79].

Magnetic nuclei can also be described in terms of their magnetogyric ratio (γ)[79] where:

$$\gamma=\mu/I\hbar$$

This ratio consists of the nuclear magnetic moment (μ) divided by the nuclear angular momentum ($I\hbar$,where $\hbar$ is the Planck constant divided

by 2π). Since the magnetic moment and the nuclear angular momentum behave as parallel vectors, the magnetogyric ratio is most commonly used to describe the magnetic properties of a particular nucleus [79].

1.3.2 Magnetic Nuclei in a Magnetic Field

Under normal conditions at thermal equilibrium dipole nuclei exhibit a random orientation in space (figure 23a). However, in the presence of a static, uniform magnetic field (H_o) these nuclei become aligned with the magnetic field (figure 23b).[89]. The equation 2I+1 describes the number of possible alignments of a magnetic nuclei in a magnetic field [79]. Thus, if the spin quantum number of the phosphorus nucleus is 1/2, it can align itself either parallel to (M_I=+1/2) or antiparallel to(M_I=-1/2) the magnetic field (figure 23b) [79].

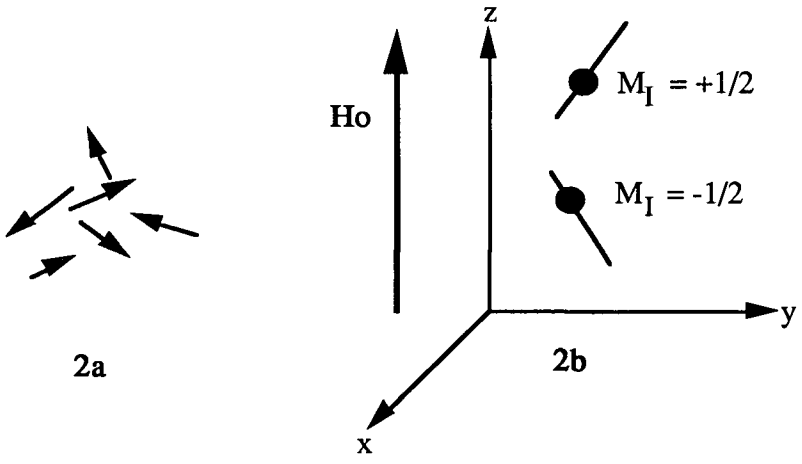

Figure 23
(adapted from Meyer)

These two alignments give rise to the two energetic states (E) of the affected nuclei [79]:

$$E=-\mu H_o \cos\theta$$

where H_o is the static magnetic field and θ is the angle between H_o and μ. Since two alignments along the z axis are possible, two distinct energy levels form:

$$E_{low} = -(1/2\gamma\hbar)H_o \text{ (parallel)}$$

$$E_{high} = -(-1/2\gamma\hbar)H_o \text{ (antiparallel)}$$

With the difference between the energy levels (ΔE) described by:

$$\Delta E = \gamma\hbar H_o$$

The energy difference between these two states is very small, thus, only a slight excess of nuclei are present in the lower energy state (figure 24)[79]. In fact, the Boltzman distribution law dictates that this excess consists of only 1 nucleus in 10,000 [79]. Thus, the capacity of a system to absorb energy by NMR is very small [73]. Considering the weak interaction between the magnetic nuclei and the applied magnetic field (H_o) the desirability of maximizing the strength of the magnetic field (and thus ΔE) becomes obvious.

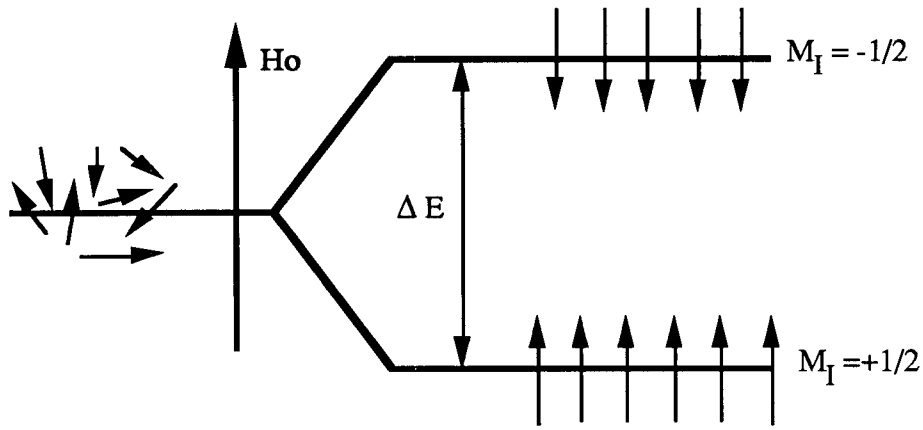

Figure 24
(adapted from Paudler)

In addition to altering nuclear alignment, the static magnetic field (H_o) also produces precession of μ in the X-Y plane about the Z axis (in the direction of H_o) (figure 25) [79].

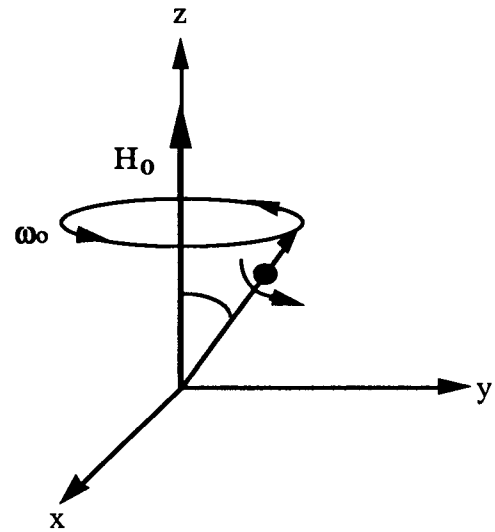

Figure 25
(Adapted from Paulder)

The frequency of precession (ω_o) is related to the strength of H_o and the magnetogyric ratio (γ) of the nuclei under investigation,such that:

$$\omega_o=-\gamma H_o$$

Thus, when exposed to a static magnetic field nuclei with different spin quantum numbers and magnetic moments will exhibit specific precessional frequencies. This specific frequency is referred to as the Larmor frequency [79]. Since nuclei with a 1/2 spin quantum number may align with H_o in two directions, the precession of μ may be diagrammatically represented by vectors forming two cone shapes, attached at their apices (figure 26). The sum of these individual vectors can be represented by a net magnetization vector (M). The magnitude of M is proportional to the number of a given type of nuclei in the sample under investigation [73].

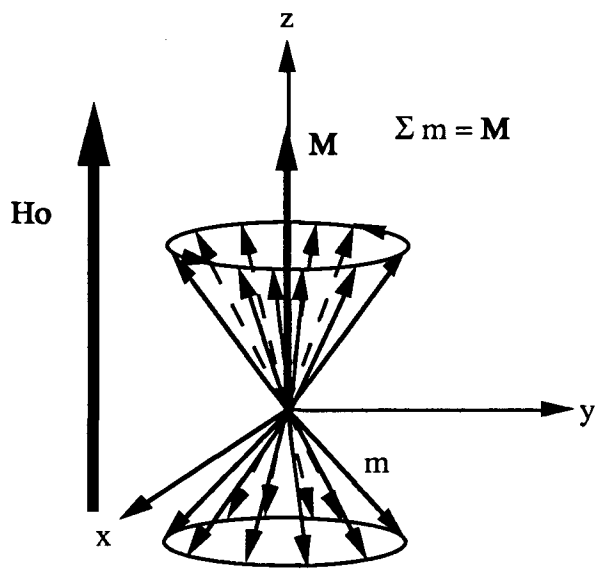

Figure 26

Application of a second, radiofrequency, magnetic field (H_1) at right angles to H_0, and rotating at the Larmor frequency, causes the nuclei to absorb energy. This absorption has a polarizing effect, and produces a rotation of M away from H_0 towards the XY plane [73]. This rotation can be diagrammatically represented in a coordinate frame, also rotating at the Larmor frequency, by a vector H_1 directed along the X axis, producing movement of vector M away from the Z axis towards the Y axis (figure 27).

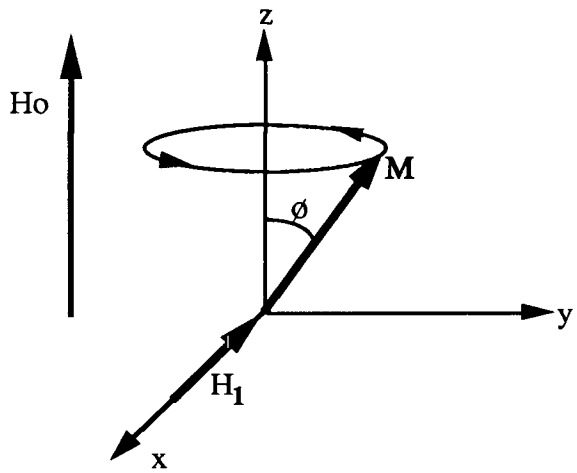

Figure 27

The H_1 magnetic field is generated by passing radiofrequency current through a coil shaped wire [73]. Maximum interaction between H_1 and the dipole nuclei occurs when the frequency of H_1 equals the Larmor frequency [79]. When the frequency of H_1 is equal to the Larmor

frequency (ω_o), the RF pulse produces precession of M ,in the Z-Y plane, about H_1 (Figure 28 [2]).

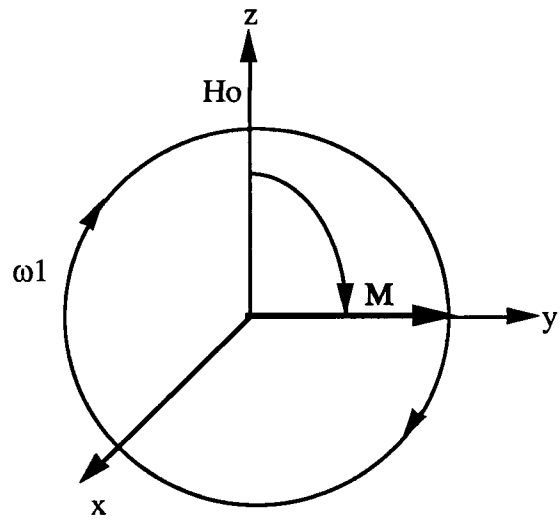

Figure 28
(from Albo)

In turn the angular frequency of precession of X-Y component of M about the H_1 (X) axis is given by:

$$\omega_1=-\gamma H_1$$

The degree of rotation of M away from H_o is dependant on the length of time for which the H_1 pulse is applied [73]. The final angle of rotation ø is given by:

$$ø=\gamma H_1 t$$

where t is the length of the RF pulse [79]. Thus, an RF pulse producing rotation of M to the XY plane is termed the 90 degree excitation pulse (figure 29)[73].

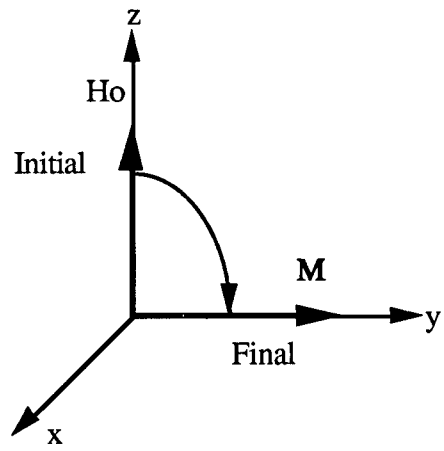

Figure 29

The behavior of the magnetic nuclei as they return to a resting alignment with H_o following an RF pulse is the basis for the formation of an NMR spectrum. After cessation of the RF pulse some component of the net magnetization vector M will persist in the X-Y plane and precess, about the Z axis, at the Larmor frequency ω_o [73]. This precession causes a magnetic field to induce an electromotive force in the RF coil. The magnitude of this induced AC voltage is proportional to the magnitude of M_{xy} and the frequency ω_o [19, 89]. The same RF coil used to produce the H_1 magnetic field may be used to collect the AC signal produced by M_{xy}. Since the Larmor frequency is specific to a type of nucleus the RF coil may the 'tuned' to receive signals from a specific type of nucleus within the magnetic field Ho [73]. This electrical signal is then amplified and processed to produce an NMR spectrum [19].

As the RF signal is collected the XY component of the net magnetization vector M decays to zero [15]. At the same time, though

not necessarily at the same rate, the Z component increased to its equilibrium value (parallel to H_0)[15]. The first of these processes causes the amplitude of the RF signal to gradually decline or 'decay' [73]. Thus, a raw NMR signal collected over time is termed free induced decay (FID)(figure 30)[19]. This time domain signal is then subjected to a mathematical process, known as Fourier transformation, which converts temporal signals to signals in the frequency domain [79]. Fourier transformation of the FID produces a frequency spectrum (Figure 31) containing the magnitude of each resonance (y axis) and its frequency, relative to an arbitrary zero point, measured in ppm of the magnetic field H_0 on the x axis [15].

1.3.3 Relaxation

The disturbance of nuclear alignment which results from the RF pulse H_1 may be separated into two components [73]. The movement of M into the X-Y plane eliminates the random distribution of individual dipoles in the X-Y plane [73]. In addition, M is no longer aligned with the z axis. Thus, as a group, the dipole nuclei are no longer distributed, in accordance with the Boltzman equilibrium distribution, between two energy levels (E_{high}/E_{low}). The process which produces the return of M to its former parallel alignment with Z is referred to as longitudinal, or spin-lattice, relaxation [15, 73].

The return of the dipole nuclei to a random distribution in the X-Y plane is referred to as transverse, or spin-spin, relaxation [15]. As these nuclear moments randomize about the Z axis in the X-Y plane, they produce signals with a spread of frequencies within the RF coil. This results in the production of a resonance peak encompassing a small

range of frequencies, as opposed to a thin single frequency line [73]. The faster this relaxation occurs, the broader the base of the spectral peak [15]. Complete transverse relaxation is characterized by a return to complete randomization in the X-Y plane. Longitudinal relaxation (T_1) is either equal to, or longer than, transverse relaxation (T_2). This time difference often resulting in complete decay of the M_{xy} signal before M is realigned with Z [73].

Local magnetic and molecular environments have a significant effect of transverse relaxation time, and therefore on the spectral signal [73, 79]. Generally speaking lower molecular mobility results in a faster transverse relaxation time [73]. Thus unbound intracellular molecules like phosphocreatine exhibit long relaxation times, and are easily seen on skeletal muscle spectra. In contrast, adenosine diphosphate (ADP) bound to actin exhibits a peak too broad to observe without special hardware [73].

Spectral signals obtained following an RF pulse will only be proportional to the number of nuclei in the interrogated sample if the system was in equilibrium prior to the application of the RF pulse [73]. If the rate of pulse application is greater than the relaxation time the resulting inability of the nuclei to return to their resting state prior to the next pulse is termed nuclear saturation [15]. Nuclear saturation is commonly induced when pulse intervals shorter than T_1 are employed during NMRS investigations of working skeletal muscle. When saturation occurs correction factors must be applied to the data, since the initial state of the nuclei effect their response to the subsequent RF pulse [15]. These correction factor may be established by measuring

stable metabolites with the same RF uptake coil utilized during data collection [73].

1.3.4 The Chemical Shift

The position of a resonance peak on the x axis of a NMR spectrum is dictated by the resonance frequency of that nucleus, expressed in ppm, relative to an arbitrary zero point [38]. The separation between each resonance peak and this zero point is termed the chemical shift. The resonance frequency is proportional to the local magnetic field (H_{local}) experienced by the nucleus [38]. Several factors effect the H_{local} experienced by a particular nucleus, induced by a given H_o.

Application of a static magnetic field (H_o) induces electronic currents in atoms and molecules. The resulting small electronic field (H_σ), produced by charged particles surrounding the nucleus, is proportional to H_o. Thus, the effective field at the nucleus can be written [38]:

$$H_{local} = H_o\ (1-\sigma)$$

where σ is termed the shielding constant, whose magnitude is determined by the electronic environment of the nucleus [38]. An increase in the magnitude of H_σ as a result of high electron densities close to, or electron donating groups adjacent to, the nucleus would decrease the magnitude of the H_{local}, resulting in a downfield shift of the nuclear resonance frequency [79]. Conversely, a decrease in this shielding effect would produce an upfield shift in the nuclear resonance frequency. Thus, nuclei in different chemical environments yield signals at different frequencies.

The orientation of neighboring nuclei to H_o may also effect H_{local} [79]. A net antiparallel orientation on neighboring nuclei would reduce the H_{local} of the nucleus, resulting in an downfield shift of the observed resonance frequency. In contrast, parallel orientation of neighboring nuclei increases H_{local}, resulting in an upfield shift of the nuclear frequency resonance. The effects of local nuclear environments on chemical shift is illustrated by the three resonance frequencies produced by each of the three phosphorus groups in ATP signal visualized in figure 31.

Observation of changes in resonance frequency during data collection can also prove extremely valuable. The frequency resonance of inorganic phosphate (Pi) is particularly sensitive to pH changes in the physiological range. Thus observed changes in the chemical shift between Pi and phosphocreatine (PCr) can be used to measure intracellular pH changes in vivo [38]. This method can reliably measure relative changes in intracellular pH within 0.05 pH units [38].

Figure 30
Free Induced Decay (F.I.D.)

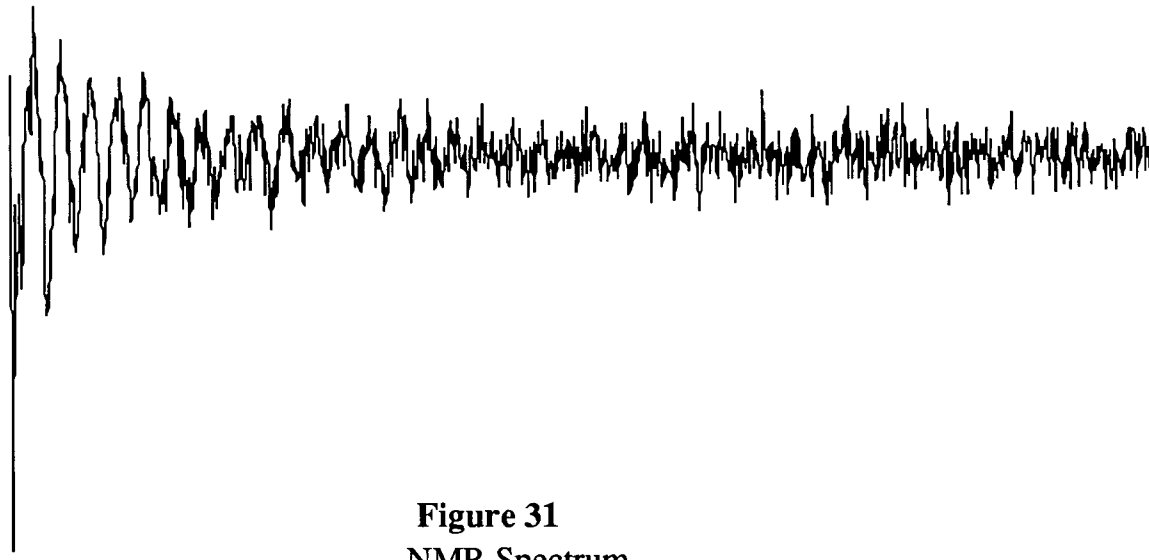

Figure 31
NMR Spectrum

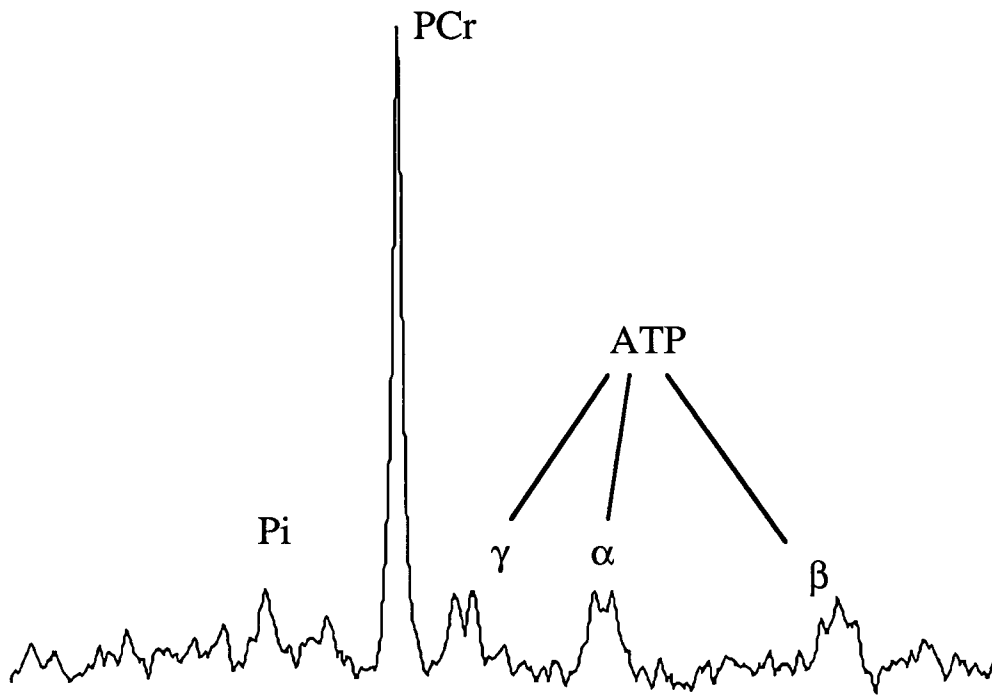

Resting NMR spectra following fourier transformation of F.I.D. (figure 9) Areas under each peak were used to calculate relative concentrations of the phosphorus metabolites labeled above.

1.3.5 Localization

Localization of the electromagnetic pulse to a specific region of tissue is achieved by utilizing a small RF surface coil, and depth pulse techniques [73]. When placed directly over the tissue to be investigated the coil produces the electromagnetic pulse required to affect the nuclei under investigation. In addition the coil receives the RF energy emitted at a specific frequency by these nuclei [19, 73]. The volume and area of the tissue interrogate is dependant on the size and shape of the RF coil [70]. Recently techniques have been developed to allow data collection from various depths within the same sample [70].

1.3.6 Limitations

In addition to its numerous attributes NMRS also possesses some limitations. NMRS is currently only capable of measuring metabolites in the millimolar concentration range [73]. This inherent insensitivity makes measurement of compounds present in very low concentrations, like adenosine monophosphate, impossible. This insensitivity also necessitates the averaging of multiple tissue scans to produce adequate spectral resolution [73]. Currently 10 -30 seconds represents the shortest scan possible during ^{31}P investigations of skeletal muscle. Localization of RF pulses by small surface coils limits data collection to a specific volume of muscle, however, it is not possible to study specific motor units or fibers with NMRS.

Currently NMR magnets are very expensive to purchase and maintain. In addition the small bore of powerful magnets has limited the study of human muscle to the forearm or leg investigations. In addition exercise in a small magnetic environment imposes inherent limitations.

Development of nonmagnetic exercise ergometers utilized through a small range of ankle or wrist motion makes whole body metabolic studies difficult.

APPENDIX 2

Raw Data

Raw data for each variable is presented in individual spread sheets, in the following format:

Row 1-5: Protocol A - Stimulation

Row 6-10: Protocol B - Stimulation

Row 11-15: Protocol A - First 10 second rest post stim.

Row 16-20: Protocol B - First 10 second rest post stim.

Row 21-25: Protocol A - First 10 second rest post stim.

Row 26-30: Protocol B - Rest period 50 seconds post stim.

Row 31-35: Protocol A - Recovery

Row 35-40: Protocol B - Recovery

Column 1-12: Stimulation 1-12 (or recovery x10 sec.)

Force Production

	A	B	C	D	E	F	G	H	I	J	K	L
1	0.99	0.898	0.897	0.878	0.877	0.847	0.817	0.794	0.78	0.767	0.773	0.738
2	0.99	0.931	0.888	0.855	0.826	0.792	0.79	0.747	0.745	0.71	0.693	0.697
3	0.95	0.912	0.918	0.862	0.782	0.772	0.723	0.767	0.731	0.691	0.719	0.741
4	0.94	0.936	0.901	0.846	0.799	0.784	0.761	0.757	0.744	0.731	0.727	0.706
5	10.95	0.856	0.798	0.706	0.667	0.665	0.64	0.627	0.615	0.609	0.584	0.577
6	0.99	0.978	0.979	0.963	0.934	0.931	0.932	0.903	0.874	0.872	0.888	0.875
7	0.98	0.975	0.957	0.955	0.939	0.932	0.933	0.924	0.907	0.911	0.909	0.913
8	0.99	0.959	0.928	0.885	0.874	0.881	0.875	0.861	0.831	0.812	0.884	0.839
9	0.94	0.958	0.892	0.868	0.853	0.852	0.851	0.86	0.823	0.795	0.861	0.857
10	20.93	0.849	0.782	0.719	0.734	0.703	0.774	0.737	0.749	0.762	0.678	0.724

Pi/PCr

	A	B	C	D	E	F	G	H	I	J	K	L
1	0.536	0.78	1.076	1.157	1.522	1.774	1.405	1.269	1.064	1.059	0.829	1.259
2	0.525	0.685	0.937	1.437	0.847	1.188	1.147	1.089	0.966	0.678	0.875	1.49
3	0.549	1.131	1.546	2.057	2.666	3.16	2.387	3.478	2.58	2.863	2.221	2.966
4	0.542	0.65	0.937	0.777	1.449	1.295	1.311	1.274	1.426	1.413	1.353	1.526
5	0.473	0.714	1.101	0.813	0.832	0.733	0.831	0.61	0.688	0.689	0.571	0.5
6	0.537	0.562	0.896	0.859	0.995	0.53	0.911	0.832	0.607	0.525	0.644	0.617
7	0.634	0.485	0.62	0.598	0.842	0.639	0.644	0.697	0.684	0.739	0.598	0.46
8	0.844	0.943	1.521	1.264	1.974	1.329	1.132	1.148	0.908	1.79	1.931	1.358
9	0.808	0.887	0.88	0.523	0.95	0.95	0.989	0.806	0.918	0.792	1.004	1.289
10	0.682	0.613	0.653	0.731	0.46	0.556	0.738	0.767	0.583	0.799	0.543	0.653
11	0.568	0.963	1.229	1.485	1.573	1.329	1.416	1.571	1.232	1.206	1.369	1.251
12	0.457	0.658	0.866	1.055	0.984	0.943	1.304	1.164	0.952	0.873	1.056	0.912
13	0.703	1.257	2.199	2.868	2.821	3.014	2.509	3.865	3.719	3.279	3.022	2.573
14	0.491	0.72	1.237	1.247	1.449	1.781	1.782	1.531	1.352	1.617	1.648	0.849
15	0.51	0.946	0.897	0.841	0.79	0.764	1.074	0.73	0.698	0.721	0.668	0.313
16	0.552	0.528	0.658	0.648	0.362	0.396	0.454	0.445	0.549	0.543	0.429	0.455
17	0.502	0.521	0.606	0.372	0.55	0.541	0.496	0.531	0.584	0.523	0.477	0.461
18	0.867	0.782	0.795	1.134	0.743	0.823	1.99	0.845	1.268	0.742	0.656	0.876
19	0.526	0.611	0.28	0.669	0.581	0.389	0.507	0.466	0.431	0.384	0.387	0.396
20	0.472	0.421	0.42	0.658	0.525	0.493	0.476	0.543	0.55	0.467	0.522	0.434
21	0.568	0.963	1.229	1.485	1.573	1.329	1.416	1.571	1.232	1.206	1.369	1.251
22	0.457	0.658	0.866	1.055	0.984	0.943	1.304	1.164	0.952	0.873	1.056	0.912
23	0.703	1.257	2.199	2.868	2.821	3.014	2.509	3.865	3.719	3.279	3.022	2.573
24	0.491	0.72	1.237	1.247	1.449	1.781	1.782	1.531	1.352	1.617	1.648	0.849
25	0.51	0.946	0.897	0.841	0.79	0.764	1.074	0.73	0.698	0.721	0.668	0.313
26	0.36	0.824	0.547	0.5	0.176	0.266	0.213	0.87	0.255	0.027	0.462	0.224
27	0.502	0.336	0.334	0.233	0.184	0.251	0.25	0.194	0.846	0.318	0.211	0.256
28	0.152	0.729	0.765	1.259	0.958	0.8	1.098	1.098	0.908	0.848	1.051	0.905
29	0.096	0.224	0.28	0.391	0.338	0.807	0.407	0.473	0.259	0.394	1.138	0.473
30	0.275	0.25	0.361	0.282	0.241	0.304	0.254	0.296	0.238	0.27	0.234	0.136
31	0.825	0.624	0.956	1.148	1.054	0.034	0.254	0.113	0.165	•	•	•
32	0.572	1.671	0.241	0.19	0.339	0.134	•	•	•	•	•	•
33	2.057	1.586	1.317	0.975	1.028	0.689	0.821	0.904	0.527	1.162	•	•
34	0.785	0.625	0.402	0.402	0.439	0.29	0.253	0.206	0.236	0.171	•	•
35	0.585	0.136	0.288	0.239	0.176	•	•	•	•	•	•	•
36	0.632	0.303	0.18	0.19	0.934	0.295	0.238	0.284	0.285	0.275	•	•
37	0.268	0.186	0.165	0.269	0.104	0.243	0.335	0.173	0.189	0.202	•	•
38	1.261	1.27	0.644	1.774	1.162	1.268	0.483	0.62	0.311	0.222	•	•
39	1.364	0.421	0.333	0.259	0.341	0.173	0.177	0.138	0.303	0.139	•	•
40	0.282	0.19	0.101	0.306	0.137	0.249	0.232	0.214	0.155	0.157	•	•

pHi

	A	B	C	D	E	F	G	H	I	J	K	L
1	7.23	7.19	7.11	7.11	7.11	7.23	7.19	7.04	7.08	7.04	7.05	7.04
2	7.11	7.05	7.05	7.05	6.95	7.02	6.95	6.95	6.95	6.95	6.92	6.92
3	7.15	7.11	7.08	7.02	6.98	6.85	6.79	6.73	6.73	6.65	6.65	6.65
4	7.11	7.11	7.11	7.05	6.98	6.95	6.85	6.85	6.83	6.85	6.71	6.85
5	7.15	7.08	6.98	6.98	6.84	6.98	6.92	6.95	6.98	7.02	6.92	6.85
6	7.19	7.2	7.15	7.15	7.15	7.19	7.16	7.23	7.19	7.16	7.17	7.11
7	7.19	7.19	7.09	7.11	7.04	7.05	7.11	7.11	7.11	7.11	7.15	7.15
8	7.11	7.09	7.02	6.98	7.04	6.85	6.89	6.95	6.95	7.01	6.98	6.98
9	7.08	6.98	7.01	6.98	7.04	7.05	7.08	6.98	6.98	7.01	6.95	6.98
10	7.19	7.08	7.04	6.98	7.08	7.04	7.01	7.04	7.11	7.08	7.08	7.15
11	7.11	7.15	7.11	7.11	7.04	7.08	7.01	6.98	6.98	7.04	7.02	7.05
12	7.04	6.97	7.05	6.98	6.92	6.92	6.92	6.92	6.92	6.95	6.89	6.92
13	7.11	7.04	7.05	6.89	6.85	6.76	6.76	6.7	6.7	6.61	6.58	6.61
14	7.08	7.02	7.05	6.98	6.85	6.8	6.77	6.71	6.71	6.68	6.71	6.61
15	6.98	6.98	6.89	6.85	6.85	6.82	7.03	6.85	6.82	6.82	6.85	6.85
16	7.04	7.11	7.04	7.08	6.94	7.11	7.05	7.02	7.05	7.15	7.04	7.08
17	7.11	7.08	7.05	7.02	7.04	7.08	7.08	7.04	7.11	7.15	7.15	7.15
18	7.08	7.02	7.02	6.92	6.95	6.82	6.82	6.89	6.92	6.52	6.79	6.89
19	6.95	6.98	6.92	6.92	6.95	6.92	6.89	6.92	6.85	6.98	6.95	6.82
20	7.05	6.95	6.98	6.92	6.92	6.98	7.01	6.98	6.95	6.98	7.01	7.04
21	7.11	7.15	7.11	7.11	7.04	7.08	7.01	6.98	6.98	7.04	7.02	7.05
22	7.04	6.97	7.05	6.98	6.92	6.92	6.92	6.92	6.92	6.95	6.89	6.92
23	7.11	7.04	7.05	6.89	6.85	6.76	6.76	6.7	6.7	6.61	6.58	6.61
24	7.08	7.02	7.05	6.98	6.85	6.8	6.77	6.71	6.71	6.68	6.71	6.61
25	6.98	6.98	6.89	6.85	6.85	6.82	7.03	6.85	6.82	6.82	6.85	6.85
26	7.01	7.04	7.05	7.04	7.22	6.92	6.98	7.02	7.04	7.19	7.04	6.95
27	7.11	7.09	7.02	7.05	6.98	7.08	7.05	7.11	7.05	7.11	7.04	7.08
28	6.23	7.09	6.95	6.9	6.89	6.85	6.85	6.85	6.67	6.73	6.67	6.73
29	6.98	6.85	6.85	6.85	6.79	6.85	6.79	6.76	6.76	6.76	6.76	6.71
30	7.15	6.89	6.89	6.92	6.89	6.92	6.92	6.95	7.08	6.95	6.89	6.89
31	7.04	7.02	6.98	6.92	7.02	6.89	7.11	6.98	7.01	7.08	7.11	
32	6.92	6.73	6.85	6.82	6.73	6.89	6.61	6.77	6.89	6.85	6.85	
33	6.61	6.55	6.52	6.48	6.45	6.52	6.45	6.38	6.41	6.41	6.52	
34	6.61	6.58	6.55	6.55	6.52	6.52	6.48	6.52	6.48	6.46	7.19	
35	6.68	6.98	6.89	7.22	7.08	6.89	7.01	6.95				
36	7.08	7.01	7.04	7.01	7.11	6.95	6.98	6.95	7.04	6.95	7.04	
37	7.15	7.15	7.1	7.08	7.11	7.15	7.11	7.11	7.15	7.11	7.15	
38	6.98	6.89	6.89	6.87	6.61	6.68	6.65	6.7	6.67	6.61	6.58	
39	6.98	6.82	6.82	6.82	6.79	6.82	6.67	6.65	6.65	6.52	6.45	
40	7.15	7.04	6.98	6.98	6.98	7.05	7.02	6.92	6.98	6.95	7.15	

ATP

	A	B	C	D	E	F	G	H	I	J	K	L
1	0.106	0.179	0.231	0.207	0.15	0.142	0.179	0.27	0.227	0.181	0.092	0.205
	0.175	0.158	0.169	0.101	0.183	0.222	0.162	0.199	0.101	0.144	0.171	0.195
3	0.119	0.142	0.204	0.152	0.129	0.114	0.141	0.178	0.117	0.14	0.12	0.161
4	0.296	0.137	0.226	0.138	0.148	0.128	0.11	0.119	0.308	0.136	0.184	0.103
5	0.112	0.169	0.129	0.175	0.212	0.129	0.123	0.087	0.115	0.157	0.139	0.189
6	0.147	0.165	0.122	0.196	0.13	0.156	0.266	0.191	0.166	0.18	0.208	0.167
7	0.084	0.13	0.15	0.155	0.091	0.146	0.153	0.122	0.127	0.132	0.156	0.181
8	0.07	0.175	0.213	2657	0.128	0.242	0.156	0.123	0.37	0.209	0.52	0.156
9	0.205	0.124	0.168	0.109	0.141	0.084	0.127	0.163	0.183	0.127	0.162	0.159
10	0.107	0.173	0.145	0.102	0.158	0.092	0.138	0.093	0.116	0.187	0.147	0.103
11	0.16	0.391	0.135	0.123	0.147	0.185	0.191	0.166	0.136	0.158	0.152	0.197
12	0.138	0.221	0.272	0.167	0.173	0.183	0.236	0.274	0.205	0.167	0.109	0.102
13	0.126	0.156	0.135	0.189	0.145	0.155	0.137	0.178	0.097	0.163	0.162	0.197
14	0.165	0.159	0.143	0.116	0.163	0.116	0.125	0.117	0.099	0.211	0.175	0.125
15	0.11	0.106	0.134	0.123	0.108	0.166	0.158	0.117	0.148	0.143	0.117	0.116
16	0.188	0.21	0.129	0.136	0.139	0.232	0.279	0.177	0.192	0.132	0.154	0.136
17	0.142	0.209	0.151	0.158	0.108	0.137	0.129	0.146	0.127	0.087	0.118	0.114
18	0.162	0.182	0.199	0.142	0.273	0.263	0.113	0.217	0.11	0.113	0.17	0.218
19	0.135	0.168	0.148	0.17	0.113	0.13	0.218	0.168	0.203	0.127	0.103	0.144
20	0.114	0.127	0.132	0.17	0.1	0.155	0.119	0.097	0.152	0.154	0.092	0.142
21	0.16	0.391	0.135	0.123	0.147	0.185	0.191	0.166	0.136	0.158	0.152	0.197
22	0.138	0.221	0.272	0.167	0.173	0.183	0.236	0.274	0.205	0.167	0.109	0.102
23	0.126	0.156	0.135	0.189	0.145	0.155	0.137	0.178	0.097	0.163	0.162	0.197
24	0.165	0.159	0.143	0.116	0.163	0.116	0.125	0.117	0.099	0.211	0.175	0.125
25	0.11	0.106	0.134	0.123	0.108	0.166	0.158	0.117	0.148	0.143	0.117	0.116
26	0.104	0.215	0.158	0.136	0.171	0.234	0.335	0.114	0.218	0.21	0.128	0.168
27	0.202	0.12	0.216	0.163	0.144	0.15	0.123	0.137	0.104	0.15	0.145	0.142
28	0.164	0.211	0.239	0.142	0.123	0.289	0.168	0.11	1.034	0.242	0.124	0.145
29	0.214	0.126	0.106	0.106	0.137	0.127	0.182	0.099	0.173	0.151	0.086	0.142
30	0.151	0.15	0.104	0.118	0.123	0.108	0.178	0.132	0.153	0.192	0.144	0.173
31	0.139	0.201	0.197	0.122	0.08	0.261	0.209	0.198	0.138			
32	0.221	0.205	0.131	0.099	0.136	0.135	0.183	0.149	0.182	0.274		
33	0.11	0.134	0.127	0.152	0.174	0.163	0.12	0.127	0.139	0.111		
34	0.179	0.107	0.131	0.149	0.146	0.101	0.145	0.158	0.161	0.152		
35	0.178	0.103	0.123	0.19	0.115	0.101	0.101	0.143	0.141	0.098		
36	0.335	0.158	0.134	0.082	0.14	0.139	0.098	0.155	0.191	0.43		
37	0.13	0.209	0.138	0.167	0.119	0.164	0.112	0.128	0.112	0.129		
38	0.182	0.102	0.285	0.253	0.856	0.207	0.13	0.068	0.023	0.041		
39	0.119	0.151	0.137	0.162	0.105	0.114	0.11	0.102	0.142	0.119		
40	0.127	0.145	0.133	0.151	0.16	0.149	0.128	0.137	0.177	0.094		